

General squark flavour mixing: constraints, phenomenology and benchmarks

Karen De Causmaecker^a, Benjamin Fuks^{b,c,d}, Björn Herrmann^e, Farvah Mahmoudi^{f,g,*}, Ben O’Leary^h, Werner Porod^h, Sezen Sekmenⁱ and Nadja Strobbe^{j,k}

^a*Theoretische Natuurkunde, IIHE/ELEM and International Solvay Institutes, Vrije Universiteit Brussel, Pleinlaan 2, B-1050 Brussels, Belgium*

^b*Sorbonne Universités, UPMC Univ. Paris 06, UMR 7589, LPTHE, F-75005 Paris, France*

^c*CNRS, UMR 7589, LPTHE, F-75005 Paris, France*

^d*Institut Pluridisciplinaire Hubert Curien/Département Recherches Subatomiques, Université de Strasbourg/CNRS-IN2P3, 23 Rue du Loess, F-67037 Strasbourg, France*

^e*LAPTh, Université Savoie Mont Blanc, CNRS, 9 Chemin de Bellevue, F-74941 Annecy-le-Vieux, France*

^f*Université de Lyon, Université Lyon 1, F-69622 Villeurbanne Cedex, France; Centre de Recherche Astrophysique de Lyon, CNRS, UMR 5574, Saint-Genis Laval Cedex, F-69561, France; Ecole Normale Supérieure de Lyon, France*

^g*CERN Theory Division, Physics Department, CH-1211 Geneva 23, Switzerland*

^h*Institut für Theoretische Physik und Astrophysik, Universität Würzburg, D-97074 Würzburg, Germany*

ⁱ*Kyungpook National University, Department of Physics, Daegu, 702-701 Korea*

^j*Ghent University, Department of Physics and Astronomy, Proeftuinstraat 86, B-9000 Gent, Belgium*

^k*Fermi National Accelerator Laboratory, Batavia, 60510-5011, USA*

E-mail: karen.de.causmaecker@vub.ac.be, fuks@lpthe.jussieu.fr, herrmann@lapth.cnrs.fr, nazila@cern.ch, ben.oleary@physik.uni-wuerzburg.de, porod@physik.uni-wuerzburg.de, sezen.sekmen@cern.ch, nadja.strobbe@cern.ch

ABSTRACT: We present an extensive study of non-minimal flavour violation in the squark sector in the framework of the Minimal Supersymmetric Standard Model. We investigate the effects of multiple non-vanishing flavour-violating elements in the squark mass matrices by means of a Markov Chain Monte Carlo scanning technique and identify parameter combinations that are favoured by both current data and theoretical constraints. We then detail the resulting distributions of the flavour-conserving and flavour-violating model parameters. Based on this analysis, we propose a set of benchmark scenarios relevant for future studies of non-minimal flavour violation in the Minimal Supersymmetric Standard Model.

*Also Institut Universitaire de France, 103 boulevard Saint-Michel, 75005 Paris, France

Contents

1	Introduction	1
2	The squark sector with general flavour mixing	2
3	Setup and constraints	5
3.1	Numerical setup	5
3.2	Indirect constraints on general squark mixing	6
4	Results and discussion	9
4.1	Flavour-conserving parameters	9
4.2	Flavour-violating parameters	12
4.3	Correlations within the flavour-violating parameters	15
4.4	Squark masses and flavour decomposition	16
5	Benchmark scenarios	20
6	Conclusion	24

1 Introduction

Among all possible extensions to the Standard Model of particle physics, weak scale supersymmetry [1, 2] remains one of the most popular and best studied options. The quest for the superpartners of the Standard Model degrees of freedom is one of the hot topics of the current high-energy physics experimental programme and many search channels are hence investigated at the Large Hadron Collider (LHC) [3, 4]. Since no signal of supersymmetry has been found so far, the results have been interpreted either in terms of limits on specific setups like constrained versions of the Minimal Supersymmetric Standard Model (MSSM) or in terms of simplified model spectra inspired by the MSSM. As a result, either supersymmetric particles are constrained to reside at scales that are not reachable in proton-proton collisions at a centre-of-mass energy of 8 TeV, or the spectrum must present specific properties that allow the superpartners to evade detection as in the case of compressed supersymmetric spectra or non-minimal realizations of supersymmetry. In this work, we follow this latter guiding principle and explore to which extent deviations from the minimal flavour-violation paradigm [5–7] are allowed by current data.

In minimally flavour-violating supersymmetry, all the flavour properties of the model stem from the diagonalization of the Yukawa matrices that yields different gauge and mass bases for the (s)quarks and (s)leptons. Flavour violation is thus entirely encompassed in the CKM and PMNS matrices. There is however no theoretical motivation for the flavour structure of a supersymmetric model to be the same as in the Standard Model. For

instance, when supersymmetry is embedded in a Grand Unified framework, new sources of flavour violation could be allowed [8]. The soft supersymmetry-breaking mass and trilinear coupling matrices of the sfermions could therefore comprise non-diagonal flavour-violating entries that are not related to the CKM and PMNS matrices. We adopt such a setup, which is referred to as non-minimally flavour-violating (NMFV) supersymmetry, and study the impact of these additional flavour-violating soft terms.

In recent years, the consequences of non-minimal flavour violation in the squark sector have been investigated in various areas. NMFV effects on low-energy observables such as rare decays (see, *e.g.* Ref. [9] and references therein) or oblique parameters [10] have been considered, and the potential signatures at the LHC have been investigated [11–24]. More recently, the existing constraints on possible non-vanishing flavour-mixing parameters have been updated [25, 26]. These results have been derived under the restriction that only few off-diagonal elements of the squark mass matrices are non-zero, and that at most two of them are varied at the same time. One would however generally expect that several of the flavour-violating entries could be non-vanishing, especially if the flavour structure is generated by some mechanism at a higher scale. Consequently, a comprehensive study of the most general NMFV configuration of the MSSM, where all flavour-violating Lagrangian terms are taken into account and confronted to current data and theoretical constraints, is in order. A first step in this direction is achieved with this work.

We consider the most general mixings between second and third generation squarks. Any non-CKM induced mixing with the first generation is ignored as a result of constraints imposed by kaon data [27]. Choosing a phenomenological approach, we model the flavour-violating effects under investigation by a set of 19 free parameters defined at the TeV scale and identify, by means of a Markov Chain Monte Carlo parameter scanning technique, the regions of the parameter space that are favoured in light of current data. The rest of this paper is organised as follows. We first review in Section 2 the squark sector of the MSSM when NMFV is allowed and present our parameterisation of the effects under study. In Section 3, we describe the machinery that is employed to explore the 19-dimensional NMFV MSSM parameter space and present the experimental constraints that are imposed. Our results are discussed in Section 4, we propose NMFV MSSM benchmark scenarios for the LHC Run II in Section 5 and our conclusions are given in Section 6.

2 The squark sector with general flavour mixing

Starting from the most general MSSM Lagrangian, the super-CKM basis is defined by rotating the quark and squark superfields in flavour space in a way in which the quark mass matrices m_u and m_d are diagonal. Squark and quark flavours are thus aligned, although the squark mass matrices are not necessarily diagonal. In the $(\tilde{u}_L, \tilde{c}_L, \tilde{t}_L, \tilde{u}_R, \tilde{c}_R, \tilde{t}_R)$ and $(\tilde{d}_L, \tilde{s}_L, \tilde{b}_L, \tilde{d}_R, \tilde{s}_R, \tilde{b}_R)$ bases, the up-type and down-type squark mass matrices \mathcal{M}_u^2 and

\mathcal{M}_d^2 are given by

$$\begin{aligned}\mathcal{M}_u^2 &= \begin{pmatrix} V_{\text{CKM}} M_{\tilde{Q}}^2 V_{\text{CKM}}^\dagger + m_u^2 + D_{\tilde{u},L} & \frac{v_u}{\sqrt{2}} T_u^\dagger - m_u \frac{\mu}{\tan\beta} \\ \frac{v_u}{\sqrt{2}} T_u - m_u \frac{\mu^*}{\tan\beta} & M_{\tilde{U}}^2 + m_u^2 + D_{\tilde{u},R} \end{pmatrix}, \\ \mathcal{M}_d^2 &= \begin{pmatrix} M_{\tilde{Q}}^2 + m_d^2 + D_{\tilde{d},L} & \frac{v_d}{\sqrt{2}} T_d^\dagger - m_d \mu \tan\beta \\ \frac{v_d}{\sqrt{2}} T_d - m_d \mu^* \tan\beta & M_{\tilde{D}}^2 + m_d^2 + D_{\tilde{d},R} \end{pmatrix},\end{aligned}\tag{2.1}$$

respectively. In these notations, we have introduced the soft supersymmetry-breaking squark mass matrices $M_{\tilde{Q}}^2$, $M_{\tilde{U}}^2$ and $M_{\tilde{D}}^2$ for left-handed, up-type right-handed and down-type right-handed squarks respectively, as well as the matrices T_u and T_d that embed the trilinear soft interactions of the up-type and down-type squarks with the Higgs sector. While these five matrices are defined to be flavour diagonal in usual constrained versions of the MSSM, our NMFV framework allows them to be general and possibly flavour-violating. Moreover, V_{CKM} stands for the CKM matrix, μ denotes the superpotential Higgs(ino) mass parameter and $\tan\beta = \frac{v_u}{v_d}$ is the ratio of the vacuum expectation values of the neutral components of the two Higgs doublets. Finally, the squark mass matrices also include (flavour-diagonal) D -term contributions

$$D_{\tilde{q},L} = m_Z^2 (I_q - e_q \sin^2 \theta_W) \cos 2\beta \quad \text{and} \quad D_{\tilde{q},R} = m_Z^2 e_q \sin^2 \theta_W \cos 2\beta, \tag{2.2}$$

where m_Z is the Z -boson mass, θ_W is the weak mixing angle and e_q and I_q (with $q = u, d$) are the electric charge and the weak isospin quantum numbers of the (s)quarks.

In order to reduce the number of supersymmetric input parameters, we assume that the first two generations of squarks are degenerate so that the (flavour-conserving) soft masses are determined by six free parameters,

$$\begin{aligned}(M_{\tilde{Q}})_{11} &= (M_{\tilde{Q}})_{22} \equiv M_{\tilde{Q}_{1,2}}, & (M_{\tilde{Q}})_{33} &\equiv M_{\tilde{Q}_3}, \\ (M_{\tilde{U}})_{11} &= (M_{\tilde{U}})_{22} \equiv M_{\tilde{U}_{1,2}}, & (M_{\tilde{U}})_{33} &\equiv M_{\tilde{U}_3}, \\ (M_{\tilde{D}})_{11} &= (M_{\tilde{D}})_{22} \equiv M_{\tilde{D}_{1,2}}, & (M_{\tilde{D}})_{33} &\equiv M_{\tilde{D}_3}.\end{aligned}\tag{2.3}$$

Moreover, we define the diagonal components of the trilinear couplings T_q relatively to the Yukawa matrices Y_q ,

$$(T_q)_{ii} = (A_q)_{ii} (Y_q)_{ii}. \tag{2.4}$$

We then neglect the first and second generation Yukawa couplings so that only the trilinear coupling parameters related to third generation squarks are considered as free parameters. We take them equal for simplicity, so that we have

$$(A_u)_{33} \equiv A_t, \quad (A_d)_{33} \equiv A_b \quad \text{and} \quad A_t = A_b \equiv A_f. \tag{2.5}$$

We now turn to the off-diagonal elements of the squark mass matrices. In order to be compliant with kaon data, we ignore any mixing involving one of the first generation squarks [27]. Next, following standard prescriptions [28], we normalise the remaining non-diagonal entries of the squared squark mass matrices with respect to the diagonal ones and

parameterise all considered NMFV effects by seven dimensionless quantities

$$\begin{aligned}
\delta_{LL} &= \frac{(M_{\tilde{Q}}^2)_{23}}{(M_{\tilde{Q}})_{22}(M_{\tilde{Q}})_{33}} , & \delta_{RR}^u &= \frac{(M_{\tilde{U}}^2)_{23}}{(M_{\tilde{U}})_{22}(M_{\tilde{U}})_{33}} , & \delta_{RR}^d &= \frac{(M_{\tilde{D}}^2)_{23}}{(M_{\tilde{D}})_{22}(M_{\tilde{D}})_{33}} , \\
\delta_{RL}^u &= \frac{v_u}{\sqrt{2}} \frac{(T_u)_{23}}{(M_{\tilde{Q}})_{22}(M_{\tilde{U}})_{33}} , & \delta_{LR}^u &= \frac{v_u}{\sqrt{2}} \frac{(T_u)_{32}}{(M_{\tilde{Q}})_{33}(M_{\tilde{U}})_{22}} , & & \\
\delta_{RL}^d &= \frac{v_d}{\sqrt{2}} \frac{(T_d)_{23}}{(M_{\tilde{Q}})_{22}(M_{\tilde{D}})_{33}} , & \delta_{LR}^d &= \frac{v_d}{\sqrt{2}} \frac{(T_d)_{32}}{(M_{\tilde{Q}})_{33}(M_{\tilde{D}})_{22}} . & &
\end{aligned} \tag{2.6}$$

The physical squark states \tilde{u}_i and \tilde{d}_i (with $i = 1, \dots, 6$) are obtained by diagonalizing the squared squark mass matrices $\mathcal{M}_{\tilde{u}}^2$ and $\mathcal{M}_{\tilde{d}}^2$ according to

$$\text{diag}(m_{\tilde{q}_1}^2, m_{\tilde{q}_2}^2, \dots, m_{\tilde{q}_6}^2) = \mathcal{R}_{\tilde{q}} \mathcal{M}_{\tilde{q}}^2 \mathcal{R}_{\tilde{q}}^\dagger \quad \text{for } q = u, d . \tag{2.7}$$

By convention the mass eigenstates are taken ordered such that $m_{\tilde{q}_1}^2 < \dots < m_{\tilde{q}_6}^2$. The 6×6 rotation matrices $\mathcal{R}_{\tilde{u}}$ and $\mathcal{R}_{\tilde{d}}$ carry the information about the flavour decomposition of the squarks,

$$\begin{aligned}
(\tilde{u}_1 \ \tilde{u}_2 \ \tilde{u}_3 \ \tilde{u}_4 \ \tilde{u}_5 \ \tilde{u}_6)^t &= \mathcal{R}_{\tilde{u}} (\tilde{u}_L \ \tilde{c}_L \ \tilde{t}_L \ \tilde{u}_R \ \tilde{c}_R \ \tilde{t}_R)^t , \\
(\tilde{d}_1 \ \tilde{d}_2 \ \tilde{d}_3 \ \tilde{d}_4 \ \tilde{d}_5 \ \tilde{d}_6)^t &= \mathcal{R}_{\tilde{d}} (\tilde{d}_L \ \tilde{s}_L \ \tilde{b}_L \ \tilde{d}_R \ \tilde{s}_R \ \tilde{b}_R)^t ,
\end{aligned} \tag{2.8}$$

and their different entries directly appear in couplings of the squarks to the other particles (see, *e.g.* Refs. [11, 18]).

In addition, the gaugino sector is chosen to be determined by a single parameter, the bino mass M_1 . The wino and gluino tree-level masses M_2 and M_3 are then obtained by making use of a relation inspired by Grand-Unified theories,

$$M_1 = \frac{1}{2} M_2 = \frac{1}{6} M_3 . \tag{2.9}$$

The slepton sector is defined in a flavour-conserving fashion, so that the soft terms consist of three (diagonal) mass parameters that we set to a common value

$$(M_{\tilde{\ell}})_{11} = (M_{\tilde{\ell}})_{22} = (M_{\tilde{\ell}})_{33} \equiv M_{\tilde{\ell}} , \tag{2.10}$$

and the slepton trilinear coupling matrix to the Higgs sector T_ℓ contains a single non-zero entry,

$$(T_\ell)_{33} = Y_\tau A_\tau \equiv Y_\tau A_f . \tag{2.11}$$

All flavour-conserving trilinear sfermion interactions with the Higgs bosons are consequently driven by a single input parameter A_f . The model description is completed by the definition of the Higgs sector that is parameterised in terms of the μ parameter, $\tan \beta$ and the pole mass of the pseudoscalar Higgs boson m_A .

Parameter	Value	Parameter	Value
$\alpha^{-1}(m_Z)$	127.934	m_e	510.9989 keV
m_Z	91.1876 GeV	m_μ	105.6583 MeV
G_F	$1.16637 \times 10^{-5} \text{ GeV}^{-2}$	m_τ	1.77699 GeV
$m_c^{\overline{\text{MS}}}(m_c)$	1.25 GeV	λ^{CKM}	0.2272
$m_s^{\overline{\text{MS}}}(2 \text{ GeV})$	120 MeV	A^{CKM}	0.818
$m_u^{\overline{\text{MS}}}(2 \text{ GeV})$	3 MeV	$\bar{\rho}^{\text{CKM}}$	0.221
$m_d^{\overline{\text{MS}}}(2 \text{ GeV})$	7 MeV	$\bar{\eta}^{\text{CKM}}$	0.34

Table 1. Standard Model sector of our NMFV MSSM parameter space.

3 Setup and constraints

3.1 Numerical setup

In the previous section, we have defined a simplified parameterisation of general NMFV MSSM scenarios in terms of 16 soft supersymmetry-breaking parameters to which we have supplemented three parameters related to the Higgs sector. Turning to the Standard Model sector, the QCD interaction strength is computed from the value of the strong coupling constant at the Z -pole $\alpha_s(m_Z)$, while we choose as three independent electroweak inputs the electromagnetic coupling constant evaluated at the Z -pole $\alpha(m_Z)$, the Fermi constant G_F and the Z -boson mass m_Z . The fermion sector is defined by the pole mass of the top quark m_t^{pole} , the $\overline{\text{MS}}$ mass of the bottom (charm) quark m_b (m_c) evaluated at the m_b (m_c) scale and the $\overline{\text{MS}}$ masses of the three lightest quarks evaluated at a scale of 2 GeV. Finally, we include in our parameterisation the masses of the electron (m_e), the muon (m_μ) and the tau (m_τ) and we calculate the CKM matrix using the Wolfenstein parameters λ^{CKM} , A^{CKM} , $\bar{\rho}^{\text{CKM}}$ and $\bar{\eta}^{\text{CKM}}$.

For our exploration of the NMFV MSSM, we start by fixing the Standard Model parameters to the values provided in the review of the Particle Data Group [29], as shown in Table 1. We then allow $\alpha_s(m_Z)$, m_t^{pole} and $m_b^{\overline{\text{MS}}}(m_b)$ to vary according to Gaussian profiles with their measured central values and errors taken as means and widths, as shown in Table 2. We vary randomly all the 19 supersymmetric parameters in the intervals presented in this table and finally calculate the resulting mass spectrum of the supersymmetric particles at the one-loop level using the publicly available spectrum generator **SPheno** [30, 31]. We can in this way widely cover the regions of the parameter space where the electroweak symmetry is successfully broken (with, *e.g.* sub-TeV values for the μ parameter) and whose signatures are in principle observable at the LHC within the next few years (*i.e.* with not dramatically large soft sfermion masses). Moreover, the trilinear coupling parameter A_f and the δ -parameters have been chosen to prevent all off-diagonal elements of the squark mass matrices from being too large, so that tachyonic mass-eigenstates are avoided.

In order to explore the 22-dimensional parameter space summarized in Table 2, we

Parameter	Scanned range	Parameter	Scanned range
$\alpha_s(m_Z)$	$\mathcal{N}(0.1184, 0.0007)$	$\tan \beta$	[10, 50]
m_t^{pole}	$\mathcal{N}(173.3, 1.3928)$ GeV	μ	[100, 850] GeV
$m_b(m_b)$	$\mathcal{N}(4.19, 0.12)$ GeV	m_A	[100, 1600] GeV
$M_{\tilde{Q}_{1,2}}$	[300, 3500] GeV	M_1	[100, 1600] GeV
$M_{\tilde{Q}_3}$	[100, 3500] GeV	$M_{\tilde{\ell}}$	[100, 3500] GeV
$M_{\tilde{U}_{1,2}}$	[300, 3500] GeV	δ_{LL}	[-0.8, 0.8]
$M_{\tilde{U}_3}$	[100, 3500] GeV	δ_{RR}^u	[-0.8, 0.8]
$M_{\tilde{D}_{1,2}}$	[300, 3500] GeV	δ_{RR}^d	[-0.8, 0.8]
$M_{\tilde{D}_3}$	[100, 3500] GeV	δ_{LR}^u	[-0.5, 0.5]
A_f	[-10000, 10000] GeV or $ A_f < 4 \max\{M_{\tilde{q}}, M_{\tilde{\ell}}\}$	δ_{RL}^u	[-0.5, 0.5]
		δ_{LR}^d	[-0.05, 0.05]
		δ_{RL}^d	[-0.05, 0.05]

Table 2. Supersymmetric and Higgs sectors of our NMFV MSSM parameter space, as well as varying Standard Model parameters. $\mathcal{N}(\mu, \sigma)$ denotes a Gaussian profile of mean μ and width σ .

rely on a Markov Chain Monte Carlo (MCMC) scanning technique [32–34] and impose on each of the studied setups a set of constraints that is described in the next subsection. In this scanning procedure, a given point is accepted or rejected based on the comparison of the products of likelihoods of this point with that of the previous point, where each of the likelihoods is associated with a specific constraint accounting for measurements and theoretical predictions in the NMFV MSSM framework.

3.2 Indirect constraints on general squark mixing

The masses and flavour-violating mixings of the superpartners can be indirectly probed by numerous flavour physics constraints, the anomalous moment of the muon as well as by the properties of the recently discovered Standard-Model-like Higgs boson. In our MCMC scanning procedure, we additionally impose the lightest superpartner to be the lightest neutralino, so that it could be a phenomenologically viable dark matter candidate. We dedicate the rest of this section to a brief description of all observables that have been considered in the scan and that are summarised in Table 3.

Non-minimal flavour-violating squark mixing involving third generation squarks is by construction very sensitive to constraints arising from B -physics observables. In particular, B -meson rare decays and oscillations are expected to play an important role as the Standard Model contributions are loop-suppressed. Although we only consider squark mixing between the second and third generations, we also include constraints arising from observables related to the kaon sector. Even if not present at the scale at which we calculate the supersymmetric spectrum (*i.e.* the electroweak symmetry breaking scale), squark mixings with

Observable	Experimental result	Likelihood function
$\text{BR}(B \rightarrow X_s \gamma)$	$(3.43 \pm 0.22) \times 10^{-4}$ [35]	Gaussian
$\text{BR}(B_s \rightarrow \mu\mu)$	$(2.8 \pm 0.7) \times 10^{-9}$ [36]	Gaussian
$\text{BR}(B \rightarrow K^* \mu\mu)_{q^2 \in [1,6]} \text{ GeV}^2$	$(1.7 \pm 0.31) \times 10^{-7}$ [37]	Gaussian
$\text{AFB}(B \rightarrow K^* \mu\mu)_{q^2 \in [1.1,6]} \text{ GeV}^2$	$(-0.075 \pm 0.036) \times 10^{-7}$ [38]	Gaussian
$\text{BR}(B \rightarrow X_s \mu\mu)_{q^2 \in [1,6]} \text{ GeV}^2$	$(0.66 \pm 0.88) \times 10^{-6}$ [39]	Gaussian
$\text{BR}(B \rightarrow X_s \mu\mu)_{q^2 > 14.4} \text{ GeV}^2$	$(0.60 \pm 0.31) \times 10^{-6}$ [39]	Gaussian
$\text{BR}(B_u \rightarrow \tau\nu)/\text{BR}(B_u \rightarrow \tau\nu)_{\text{SM}}$	1.04 ± 0.34 [29]	Gaussian
ΔM_{B_s}	$(17.719 \pm 3.300) \text{ ps}^{-1}$ [29]	Gaussian
ϵ_K	$(2.228 \pm 0.29^{\text{th}}) \times 10^{-3}$ [29]	Gaussian
$\text{BR}(K^0 \rightarrow \pi^0 \nu\nu)$	$\leq 2.6 \times 10^{-8}$ [29]	1 if yes, 0 if no
$\text{BR}(K^+ \rightarrow \pi^+ \nu\nu)$	$1.73_{-1.05}^{+1.15} \times 10^{-10}$ [29]	Two-sided Gaussian
Δa_μ	$(26.1 \pm 12.8) \times 10^{-10} [e^+ e^-]$ [29]	Gaussian
m_h	$125.5 \pm 2.5 \text{ GeV}$ [40, 41]	1 if yes, 0 if no
Lightest supersymmetric particle	Lightest neutralino	1 if yes, 0 if no

Table 3. Experimental constraints imposed in our scan of the NMFV MSSM parameter space.

the first generation are induced by the non-vanishing CKM matrix and renormalisation-group running so that kaon physics observables (calculated at a different scale) are also relevant for extracting constraints on the NMFV MSSM parameter space.

We focus on the branching ratios associated with the rare $B \rightarrow X_s \gamma$, $B \rightarrow K^* \mu\mu$, $B \rightarrow X_s \mu\mu$ and $B_u \rightarrow \tau\nu$ decays, as well as on the forward-backward asymmetry (AFB) arising in $B \rightarrow K^* \mu\mu$ decays. The associated predictions are calculated with the **SuperIso** package [42, 43]. In addition, we compute the neutral B -meson mass difference ΔM_{B_s} , the branching ratio associated with the $B_s \rightarrow \mu^+ \mu^-$, $K^0 \rightarrow \pi^0 \nu\nu$ and $K^+ \rightarrow \pi^+ \nu\nu$ decays and the kaon parameter ϵ_K with the **SPheno** code [30, 31]. We furthermore employ **SPheno** for the estimation of the supersymmetric contributions to the anomalous magnetic moment of the muon a_μ ¹ and for a calculation of the lightest Higgs boson mass m_h . The data transfer between **SPheno** and **SuperIso** is achieved through the Flavour Les Houches Accord standard [44], and the Wilson coefficients for all hadronic observables are calculated in **SPheno** (at the scale $Q = 160 \text{ GeV}$) and **SuperIso** (at a scale $Q = m_W$) from the values of the running coupling constants and the supersymmetric masses and parameters that have been evaluated with **SPheno**.

We now briefly collect all references where the formulas that have been employed for the calculation of the considered observables can be found, and we indicate which NMFV

¹Imposing predictions for a_μ to agree with the related measured values leads to a preference for a lighter slepton mass spectrum. This can indirectly imply constraints on the NMFV MSSM parameters *via* the flavour observables that involve sleptons.

MSSM parameters are mainly constrained by each of these observables. The calculation of the $B \rightarrow X_s \gamma$ branching ratio is mainly based on the results of Refs. [45–47], while those of the $B \rightarrow X_s \mu^+ \mu^-$ and $B \rightarrow K^* \mu^+ \mu^-$ branching ratios respectively follow Refs. [48–51] and Refs. [52–57]. All three decays are sensitive to the left-left and to the left-right squark mixing parameters.

In the case of the $B_s \rightarrow \mu^+ \mu^-$ branching ratio, the formulas of Ref. [58] have been used. For large values of $\tan \beta$, the pseudoscalar Higgs boson contribution gives a sizeable deviation from the Standard Model expectation so that when non-minimal flavour violation in the squark sector is allowed, this observable mainly restricts left-right mixing parameters [59]. Additionally, it is also sensitive to δ_{LL} and δ_{RR}^d when the gluino is not too heavy [60]. For the B -meson oscillation parameter ΔM_{B_s} , we use the formulas of Refs. [59, 61] with the hadronic parameters $\bar{P}_1^{LR} = -0.71$, $\bar{P}_2^{LR} = -0.9$, $\bar{P}_1^{SLL} = -0.37$ and $\bar{P}_1^{SLL} = -0.72$. The NMFV contributions are mainly sensitive to the $\delta_{LL} \delta_{RR}^d$, $\delta_{LR}^d \delta_{RL}^d$ and $\delta_{LR}^u \delta_{RL}^u$ products, the relative suppression and enhancement of their contributions being driven by the ratio of the chargino over the gluino mass [14, 59].

In the kaon sector, the ϵ_K observable is estimated by combining the formulas of Refs. [59, 62], the loop-contributions being evaluated with $\eta_{tt} = 0.5$, $\eta_{ct} = 0.47$ and $\eta_{cc} = 1.44$ [63]. In addition, we fix all hadronic parameters at the scale $Q = 2$ GeV as $B_1^{VLL} = 0.61$, $B_1^{SLL} = 0.76$, $B_2^{SLL} = 0.51$, $B_1^{LR} = 0.96$ and $B_2^{LR} = 1.2$ [62], and we set the decay constant f_K to 155.8 MeV. The quantity ϵ_K is not directly sensitive to a single NMFV MSSM parameter but will allow us to constrain $\delta_{LL,13} \delta_{RR,23}^d$ and $\delta_{LL,23} \delta_{RR,13}^d$ products (recalling that first generation squark mixings are generated by renormalisation-group running). On different lines, the branching ratios associated with the rare $K^+ \rightarrow \pi^+ \nu \nu$ and $K_L \rightarrow \pi^0 \nu \nu$ decays are calculated from the formulas given in Ref. [64] with $\kappa_L = 2.1310^{-11}$, $\kappa_+ = 5.1610^{-11}$ and $P_c = 0.39$. These observables mainly constrain the product $\delta_{LR,13}^u \delta_{LR,23}^{u*}$ as well as higher-order combinations of δ -parameters that in particular appear in gluino/down-type squark box-contributions [64, 65].

In all the calculations described above, we have used the results of Ref. [66] for calculating chirally-enhanced interaction strengths that include, *e.g.* the resummation of loop-induced holomorphic coupling effects when $\tan \beta$ and/or the sfermion-Higgs trilinear couplings are large.

As we allow for relatively light sleptons, charginos and neutralinos, we calculate the supersymmetric contributions to the anomalous magnetic moment of the muon by using the formulas of Ref. [67]. The related impact in terms of constraints on our NMFV MSSM parameter space depends on the higgsino/gaugino nature of the lighter charginos and neutralinos.

Finally, the calculation of the Higgs boson mass includes the complete one-loop contribution that embeds all possible flavour structures and that is obtained by extending the formulas of Ref. [68]. For the two-loop corrections, we have made use of the formulas of Refs. [69–74] where generation mixing is neglected so that only third generation mass parameters in the super-CKM basis are used as input parameters. Although flavour effects can shift the Higgs mass by a few GeV at the one-loop level, in particular when the product $\delta_{LR}^u \delta_{RL}^u$ is large [21, 26, 75], the two-loop effects are expected to be of one order

of magnitude smaller so that ignoring the associated flavour mixing is expected to be a reasonable approximation.

4 Results and discussion

The analysis of the results of the Markov Chain Monte Carlo scan presented in Section 2 gives us information on the regions of parameter space that are favoured by the experimental data shown in Table 3. The influence of a specific experimental result on a given parameter can be studied by comparing its theoretical prior distribution to the posterior one that is derived after imposing the related constraint. The prior distributions of all parameters are obtained from a uniform random scan in which we ignore scenarios that exhibit tachyons, where the electroweak symmetry is not successfully broken and where the lightest neutralino is not the lightest supersymmetric particle. We hence include about 1.5×10^6 theoretically accepted setups. The posterior distributions are then computed on the basis of our MCMC scan in which all the experimental constraints, except the one on the Higgs boson mass, are imposed. This scan consists of 100 chains of 6000 scenarios in which the first 900 ones (the burn-in length) are removed. The constraint on the Higgs boson mass is eventually imposed and the final posterior distributions include about 100 000 points. To estimate the importance of each observable separately, we have run a separate MCMC scan consisting of 100 chains of 2000 scenarios for each observable. After removing the burn-in length, 170 000 points remain. For each scan, the convergence test of Gelman and Rubin has been verified [76].

Although we are mainly interested in the non-minimally flavour-violating parameters defined in Eq. (2.6), we first also discuss for completeness the flavour-conserving parameters of our model description.

4.1 Flavour-conserving parameters

We start the discussion with the twelve flavour-conserving parameters of our NMFV MSSM description. Figure 1 shows their probability density distributions over the respective parameter ranges. In each panel, we display the theoretical prior (yellow area) as well as the posterior distribution (solid line), which shows the impact of all constraints given in Table 3 together.

The prior distribution of the gaugino mass parameter M_1 is centred at relatively low values of $M_1 \sim 400$ GeV and may reach values ranging up to about 1000 GeV. When imposing all considered experimental constraints, the distribution is shifted by about 100 GeV to higher values. This feature can be traced to the chargino contributions to the $B_s \rightarrow \mu\mu$ branching ratio and to the neutral B -meson mass difference ΔM_{B_s} , as we have fixed the ratios of the gaugino mass parameters M_1 and M_2 so that chargino effects are connected to M_1 .

For the trilinear coupling parameter A_f , the prior distribution is centred around zero. Large values of A_f are indeed often rejected since they can induce a large left-right squark mixing implying tachyonic states. Imposing the experimental constraints drastically changes the shape of the distribution and leads to two peaks corresponding

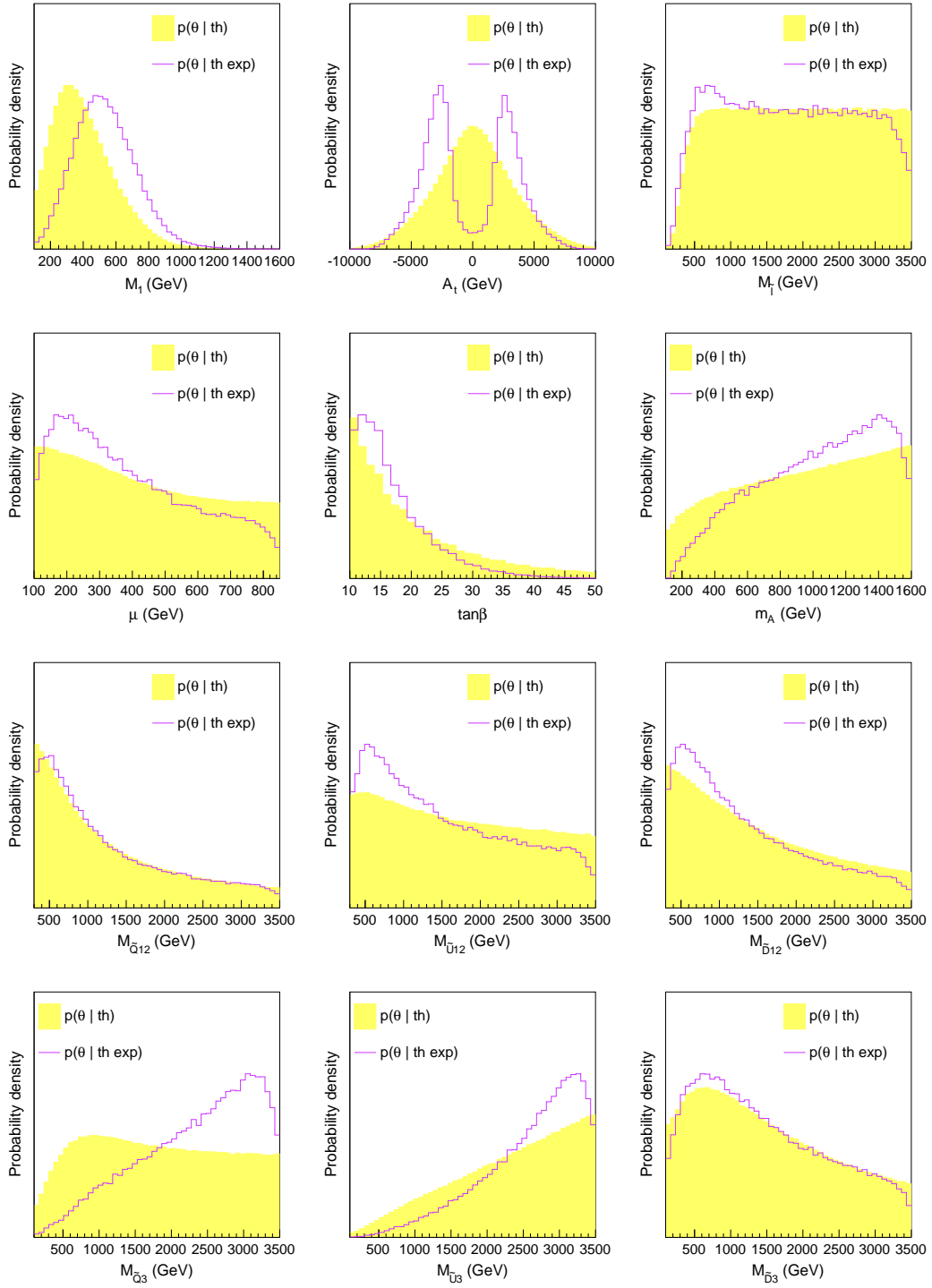


Figure 1. The one-dimensional prior (yellow histogram) and posterior (violet curve) distributions of the parameters of our NMFV MSSM description. The prior only incorporates theoretical inputs while the posterior distribution shows the impact of all experimental observations listed in Table 3.

to $|A_f| \sim 3000$ GeV. This feature is induced by the Higgs boson mass requirement that necessitates, in order to be satisfied, a relatively large splitting of the masses of the squarks exhibiting the largest stop component $m_{\tilde{q}_1}$ and $m_{\tilde{q}_2}$. More precisely, the flavour-conserving formula for the leading contributions to the Higgs mass,

$$m_h^2 = m_Z^2 \cos^2 2\beta + \frac{3g^2 m_t^4}{8\pi m_W^2} \left[\log \frac{M_{\text{SUSY}}^2}{m_t^2} + \frac{X_t^2}{M_{\text{SUSY}}^2} \left(1 - \frac{X_t^2}{12M_{\text{SUSY}}^2} \right) \right], \quad (4.1)$$

where $X_t = A_t - \mu/\tan\beta$ and $M_{\text{SUSY}}^2 = m_{\tilde{q}_1} m_{\tilde{q}_2}$, stays approximatively valid in the NMFV regime, so that peaks defined by $|X_t| \sim \sqrt{6}M_{\text{SUSY}}$ are expected (see, *e.g.* Ref. [74] and references therein).

Moving on with the slepton mass parameter $M_{\tilde{L}}$, we observe a peak centred at around 600 GeV after imposing all experimental constraints. This is mainly inferred by the anomalous magnetic moment of the muon requirement that strongly depends on the slepton sector properties. Turning to the Higgs sector (second line of Figure 1), the prior distribution of the μ -parameter shows a preference for low values while its posterior distribution slightly peaks around $\mu \sim 200$ GeV due to the $B_s \rightarrow \mu\mu$, Δa_μ and ΔM_{B_s} constraints which all depend on the chargino and neutralino sector. Next, the $\tan\beta$ parameter tends towards lower values both in its prior and posterior distributions, the favourite values being pushed to satisfy $12 \lesssim \tan\beta \lesssim 18$. Finally, the posterior distribution of the mass of the pseudoscalar Higgs boson m_A is shifted towards higher values with respect to its prior distribution. This results from the interplay of most considered observables for which low values of m_A would induce too large Higgs contributions.

The last two lines of Figure 1 concern the soft squark mass parameters. Low values are preferred for the first and second generation squark masses $M_{\tilde{Q}_{1,2}}$, $M_{\tilde{U}_{1,2}}$ and $M_{\tilde{D}_{1,2}}$, a feature that is mostly caused by the Higgs boson. This behaviour can be understood from the limiting case in which $M_{\tilde{Q}_{1,2}}^2 \simeq M_{\tilde{U}_{1,2}}^2 \simeq M_{\tilde{D}_{1,2}}^2 \equiv \tilde{m}^2$. The one-loop corrections to m_h that are proportional to δ_{LR}^u are here approximatively given by [26]

$$\Delta m_h^2 = \frac{3v_u^4}{8\pi^2(v_d^2 + v_u^2)} \left[\frac{(T_u)_{23}^2}{\tilde{m}^2} \left(\frac{Y_t^2}{2} - \frac{(T_u)_{23}^2}{12\tilde{m}^2} \right) \right], \quad (4.2)$$

while the corresponding contributions of down-type squarks are obtained by replacing T_u by T_d , Y_t by Y_b and by exchanging v_u and v_d . In our parameterisation,

$$(T_u)_{23} = \frac{\sqrt{2}}{v_u} \delta_{LR}^u M_{\tilde{Q}_{1,2}} M_{\tilde{U}_3} \quad (4.3)$$

so that for non-zero δ_{LR}^u , the Higgs boson becomes tachyonic if \tilde{m}^2 is too large. Similarly, the requirement of a physical solution for the electroweak vacuum also favours lower values for $M_{\tilde{Q}_{1,2}}$. The distributions of the third-generation mass parameters $M_{\tilde{Q}_3}$ and $M_{\tilde{U}_3}$ prefer in contrast larger values due to ΔM_{B_s} and the mass of the Higgs boson constraints. Finally, both the prior and posterior distributions of the right-handed down-type squark mass $M_{\tilde{D}_3}$ prefer lower values and are in this case very similar.

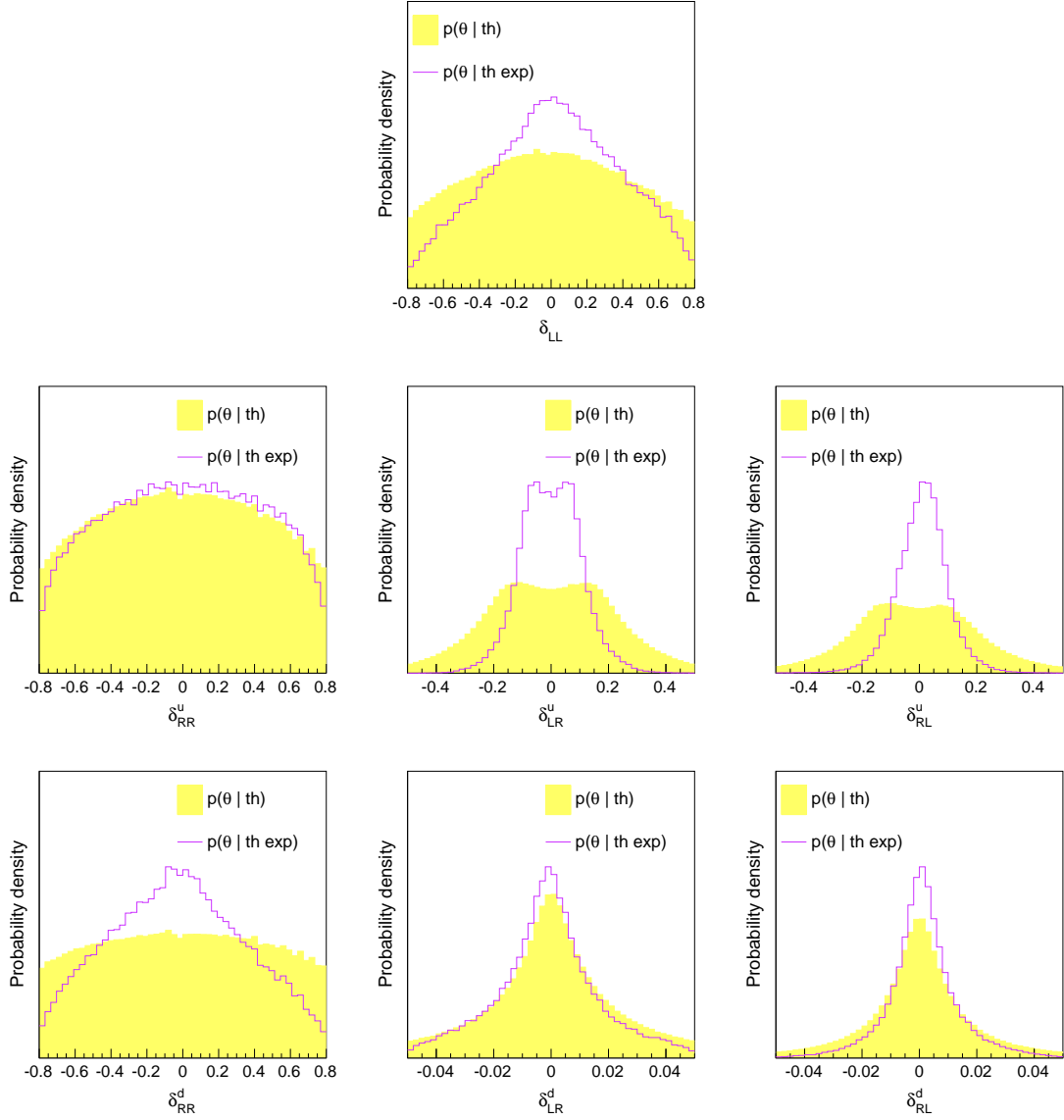


Figure 2. Same as Figure 1 in the case of the flavour-violating input parameters of our NMFV MSSM description.

4.2 Flavour-violating parameters

We now turn to the analysis of the constraints that are imposed on the seven non-minimally flavour-violating parameters $\delta_{\alpha\beta}^q$ that are at the centre of interest of the present analysis. The corresponding prior and posterior distributions are displayed in Figure 2, and we detail the impact of the most important observables on Figure 3, Figure 4 and Figure 5.

The theoretical constraints on any additional stop-scharm mixing in the left-left sector (δ_{LL}) are relatively mild such that an almost flat behaviour is observed (see Figure 2). The δ_{LL} parameter is then mainly constrained by the B -meson oscillation parameter ΔM_{B_s}

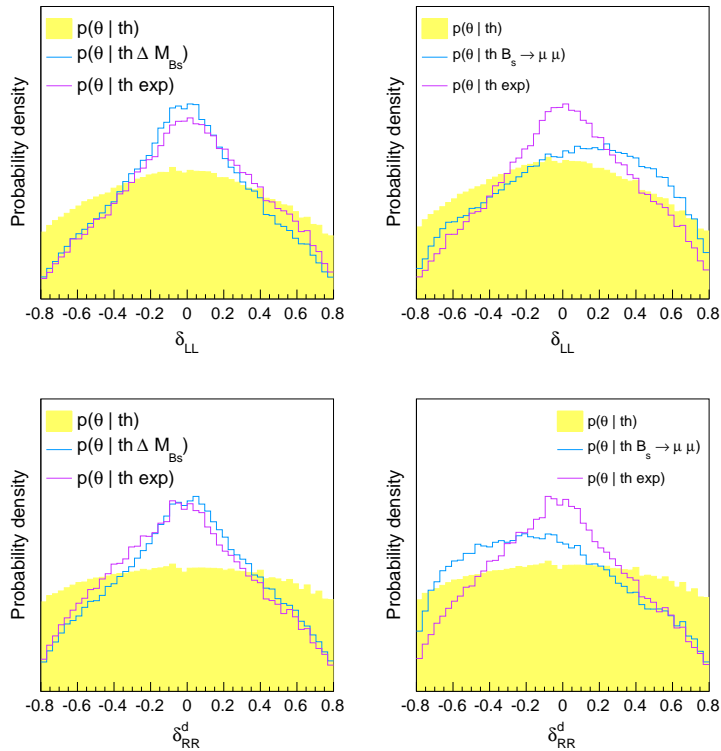


Figure 3. Most relevant observables constraining the δ_{LL} (upper panel) and δ_{RR}^d (lower panel) parameters.

(which favours smaller absolute values of δ_{LL}) and the branching ratio for the $B_s \rightarrow \mu\mu$ decay (which causes a slight preference to positive values), as shown in Figure 3. Values ranging up to $|\delta_{LL}| = 0.8$ can nevertheless be reached, but this simultaneously requires large values for other δ quantities so that cancellations between the different contributions to the considered observables occur (see Section 4.3). In a similar way, the prior distributions of the parameters δ_{RR}^u and δ_{RR}^d show a mild preference for low absolute values. The posterior distribution of the δ_{RR}^u parameter does not differ much from its prior distribution so that δ_{RR}^u is not sensitive to the experimental constraints under study. In contrast, the B -meson oscillation parameter ΔM_{B_s} restricts the posterior distribution of δ_{RR}^d to be narrower while the $B_s \rightarrow \mu\mu$ branching ratio implies a preference to negative values (see Figure 3). However, the full explored range of $-0.8 \lesssim \delta_{RR}^{u,d} \lesssim 0.8$ stays accessible in the context of both right-right mixing parameters.

The flavour-violating left-right and right-left elements of the up-type squark mass matrix (δ_{LR}^u and δ_{RL}^u) turn out to be mainly constrained by the necessity to incorporate a Higgs boson with a mass of about 125 GeV, as can be seen in Figure 4. The posterior distribution of δ_{LR}^u exhibits two peaks at $|\delta_{LR}^u| \sim 0.5$ and is restricted to $-0.15 \lesssim \delta_{LR}^u \lesssim 0.15$. Theoretically, this behaviour is expected from Eq. (4.3). The δ_{RL}^u parameter however receives extra constraints stemming from the $\text{BR}(B_s \rightarrow \mu\mu)$ observable (see Figure 4) so

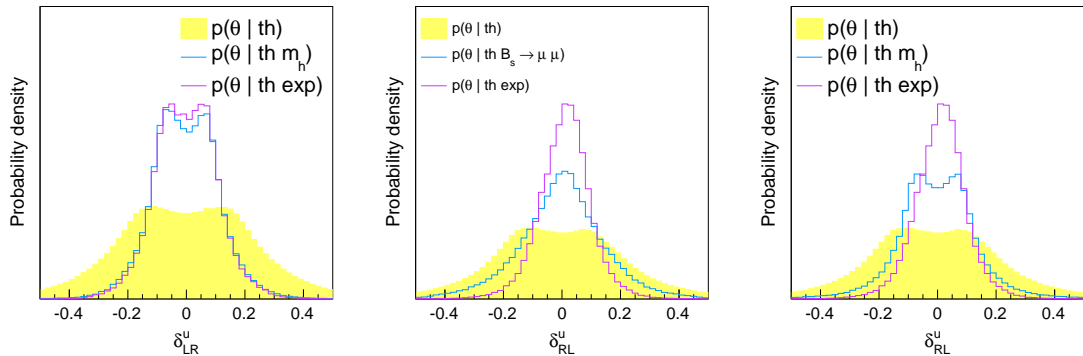


Figure 4. Most relevant observables constraining the δ_{LR}^u (left panel) and δ_{RL}^u (centre and right panel) parameters.

that the posterior distribution peaks around zero and has a maximal value of $|\delta_{RL}^u| \sim 0.2$. We recall that the two parameters δ_{LR}^u and δ_{RL}^u are independent and induce different mixing patterns. More precisely, δ_{LR}^u describes a \tilde{c}_L - \tilde{t}_R mixing, while δ_{RL}^u corresponds to mixing between the \tilde{c}_R and \tilde{t}_L eigenstates. The impact of the constraints and the resulting distributions are therefore different and directly related to the structure of the chargino-squark-quark and neutralino squark-quark interactions.

In the down-type squark sector, the prior distributions of the δ_{LR}^d and δ_{RL}^d mixing parameters show a clear peak for values close to zero. Large values are often discarded as they imply large off-diagonal terms in the $M_{\tilde{q}}$ mass matrix so that the resulting spectrum likely contains tachyons. Both parameters are hardly constrained by any of the observables under consideration and we only observe minor effects. The posterior distribution of δ_{LR}^d slightly prefers negative values, and the posterior distribution of δ_{RL}^d is slightly narrower, when both distributions are compared to their respective prior. This mostly results from an interplay of all observables, although but for the δ_{RL}^d case, the B -meson oscillation observable ΔM_{B_s} and the Higgs boson mass requirement play a non-negligible role (see Figure 5).

We now illustrate the global distribution of all NMFV parameters. To this end, we introduce the quantities

$$|\vec{\delta}| = \left[(\delta_{LL})^2 + (\delta_{RR}^u)^2 + (\delta_{RR}^d)^2 + (\delta_{LR}^u)^2 + (\delta_{RL}^u)^2 + (\delta_{LR}^d)^2 + (\delta_{RL}^d)^2 \right]^{1/2}, \quad (4.4)$$

$$\log |\Pi_\delta| = \log \left| \delta_{LL} \delta_{RR}^u \delta_{RR}^d \delta_{LR}^u \delta_{RL}^u \delta_{LR}^d \delta_{RL}^d \right|.$$

The former, $|\vec{\delta}|$, corresponds to the norm of a vector whose components are the seven NMFV parameters. Its value gives a measure of how far a given benchmark is situated from the minimally flavour-violating setup where $|\vec{\delta}| = 0$. The maximum value that can be reached in our scan is $|\vec{\delta}| \approx 1.56$. The second quantity, $\log |\Pi_\delta|$, corresponds to the logarithm of the absolute value of the product of the seven NMFV parameters. The case where all NMFV parameters are maximum corresponds to $\log |\Pi_\delta| \approx -3.5$. In Figure 6, we show the

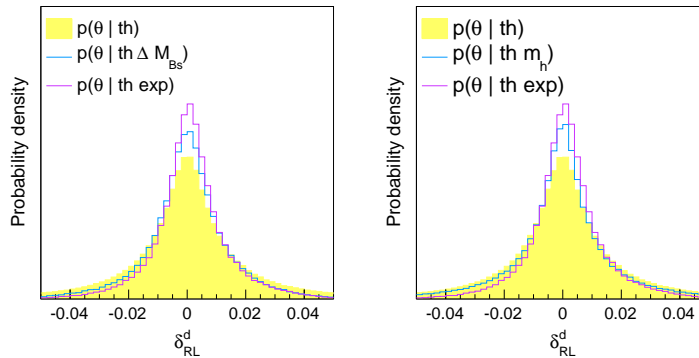


Figure 5. Most relevant observables constraining the δ_{RL}^d parameter.

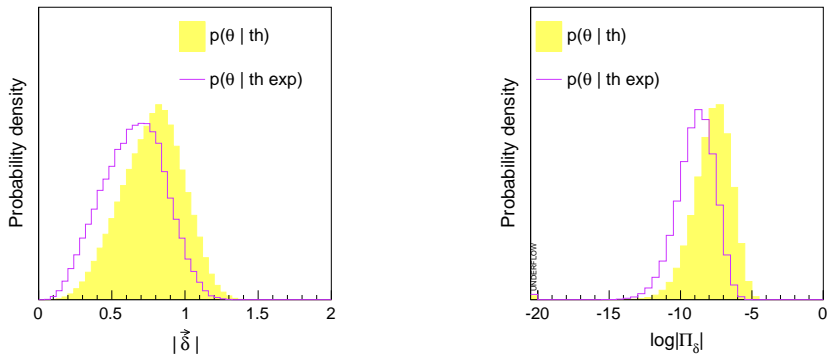


Figure 6. The one-dimensional prior (yellow histogram) and posterior (violet curve) distributions of the quantities $|\vec{\delta}|$ and $\log|\Pi_\delta|$ defined in Eq. (4.4).

prior and posterior distributions of these two quantities. All scanned points feature $|\vec{\delta}| > 0$ so that at least one of the NMFV parameters is sizeable and non-vanishing. The second quantity is in general large and negative so that at least one of the NMFV parameters has to be small. However, since the distribution shows a peak around $\log|\Pi_\delta| \approx -7$ it is clear that a large fraction of the scanned points exhibit seven non-vanishing (with some sizeable) NMFV parameters.

4.3 Correlations within the flavour-violating parameters

Having discussed the distribution of single parameters, it is interesting to investigate possible correlations between different NMFV quantities. A correlation indicator between two parameters x and y can be computed as

$$r = \frac{\sum_{i=1}^n (x_i - \bar{x})(y_i - \bar{y})}{\sqrt{\sum_{i=1}^n (x_i - \bar{x})^2} \sqrt{\sum_{i=1}^n (y_i - \bar{y})^2}}, \quad (4.5)$$

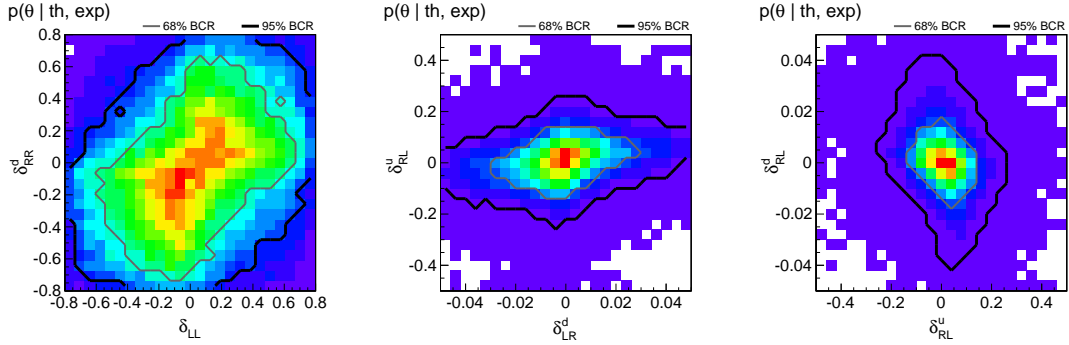


Figure 7. Two-dimensional distributions of the mostly correlated pairs of NMFV parameters after including all constraints.

where the sum runs over all the points (x_i, y_i) of the sample and \bar{x} and \bar{y} are the mean values of the two parameters. The correlation factor is vanishing when there is no correlation, while $r = \pm 1$ indicates a linear correlation with the exception of the case in which the sampled points lie on a line parallel to one of the x and y axes. As the study of the correlations only makes sense when the parameter ranges cover the entire distribution spreads, we restrict our analysis to the NMFV parameters. The correlation indicators have been computed for any pair out of the seven NMFV parameters and the results are shown in Table 4 when one only accounts for the theoretical prior (second column) and after imposing the full set of constraints (last column). The correlations are found not particularly pronounced with all r -values being close to zero.

We illustrate the correlations between different NMFV parameters on Figure 7. We however only focus on cases where the correlation indicator is above $|r| > 0.25$, namely on the $(\delta_{LL}, \delta_{RR}^d)$, $(\delta_{LR}^d, \delta_{RL}^u)$ and $(\delta_{RL}^u, \delta_{RL}^d)$ pairs. This shows that scenarios in which several NMFV parameters are non-zero (and even significantly large) simultaneously are still allowed by current low-energy flavour and Higgs data.

4.4 Squark masses and flavour decomposition

We discuss in this section the distributions of the masses of the squarks, their flavour decomposition and the mass differences between states relevant for the LHC phenomenology of NMFV MSSM models. Figure 8 shows the prior and posterior distributions for the up-type squark masses. The shapes of the distributions for the two lightest states \tilde{u}_1 and \tilde{u}_2 are very similar and they both peak at about 800–1000 GeV. The two lightest up-type states \tilde{u}_1 and \tilde{u}_2 , that are mostly of the first and second generation (see Figure 9), are in general relatively close in mass. This is due to the choice of common mass parameters for the first and second generation squarks. The heavier \tilde{u}_3 , \tilde{u}_4 and \tilde{u}_5 states exhibit more spread distributions, the masses ranging from 1 to 3.5 TeV. Finally, the heaviest state \tilde{u}_6 is barely reachable at the LHC, with a mass lying in general above 2 TeV. Although the considered experimental constraints affect all NMFV supersymmetric parameters, the associated effects on the mass eigenvalues is at the end only mild, the mass distributions being only slightly shifted towards higher values.

Parameters	th	th + exp
$(\delta_{LL}, \delta_{RR}^d)$	-0.003	0.270
$(\delta_{LR}^d, \delta_{RL}^u)$	0.007	0.267
$(\delta_{RL}^u, \delta_{RL}^d)$	-0.000	-0.254
$(\delta_{RR}^d, \delta_{RL}^u)$	-0.002	0.185
$(\delta_{LL}, \delta_{RL}^u)$	0.009	-0.158
$(\delta_{RR}^u, \delta_{RL}^u)$	0.003	-0.037
$(\delta_{LL}, \delta_{LR}^u)$	0.002	-0.031
$(\delta_{RR}^d, \delta_{LR}^d)$	-0.021	-0.028
$(\delta_{LR}^d, \delta_{RL}^d)$	-0.001	0.027
$(\delta_{LL}, \delta_{LR}^d)$	-0.002	0.023
$(\delta_{LL}, \delta_{RL}^d)$	-0.024	0.013
$(\delta_{LR}^u, \delta_{LR}^d)$	-0.006	-0.012
$(\delta_{RR}^u, \delta_{LR}^u)$	0.003	0.010
$(\delta_{RR}^u, \delta_{RL}^d)$	-0.000	-0.010
$(\delta_{RR}^d, \delta_{RL}^d)$	-0.002	-0.008
$(\delta_{LR}^u, \delta_{RL}^u)$	0.002	-0.007
$(\delta_{RR}^u, \delta_{RR}^d)$	0.001	-0.006
$(\delta_{RR}^u, \delta_{LR}^d)$	0.000	-0.003
$(\delta_{RR}^d, \delta_{LR}^u)$	-0.001	0.002
$(\delta_{LR}^u, \delta_{RL}^d)$	0.000	0.000

Table 4. The correlation coefficient r defined in Eq. (4.5) for all pairs of NMFV parameters. The parameter pairs are ordered by their correlation indicators when taking into account all imposed constraints (‘th+exp’). We also display the indicator values when only the theoretical prior is imposed (‘th’).

From a phenomenological point of view, it is interesting to examine the flavour (in particular the stop) content of the six up-type squarks. The posterior distribution of the stop content of the three lightest up-type squarks is depicted in Figure 9 and shown in correlation with the respective squark mass. The lighter states \tilde{u}_1 , \tilde{u}_2 , \tilde{u}_3 (and also \tilde{u}_4) are mainly not stop-like, *i.e.* they have a significant up or charm component. Most scanned scenarios indeed exhibit a charm-dominated lightest \tilde{u}_1 squark, while \tilde{u}_2 is mostly dominated by its up component. This contrasts with usual flavour-conserving MSSM setups where the lightest squark state is typically a stop. This feature can be traced to the first and second generation soft masses that are driven to lower values as explained in Section 4.1, whilst the third generation squark masses are pushed towards higher values by the flavour constraints. Furthermore, even in the presence of large trilinear terms, the

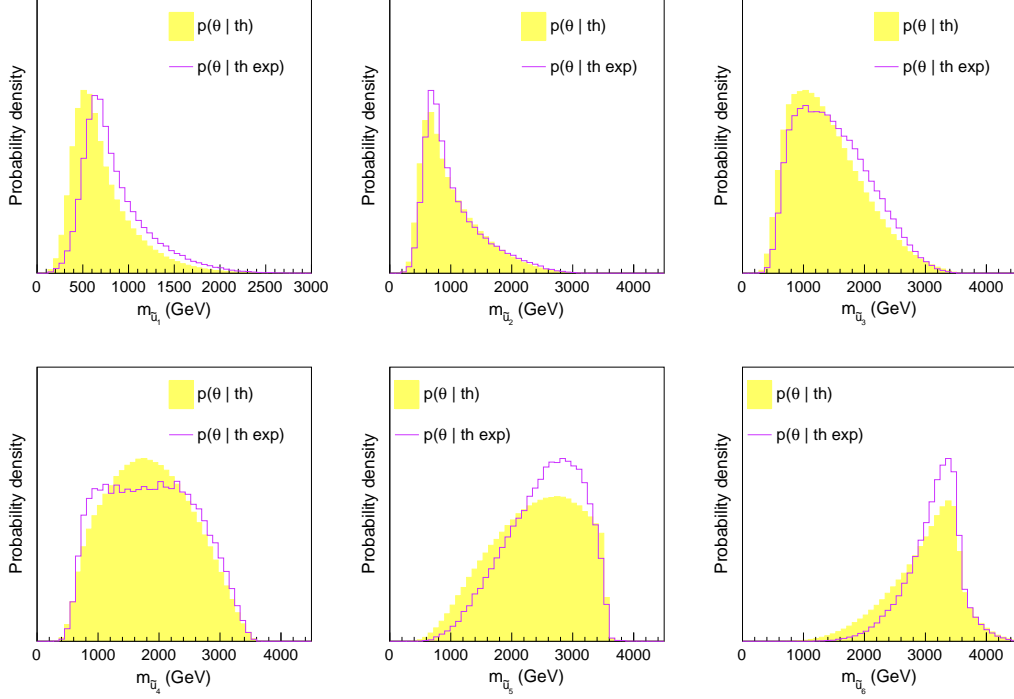


Figure 8. One-dimensional prior (yellow histogram) and posterior (violet curve) distributions of the masses of the six up-type squarks.

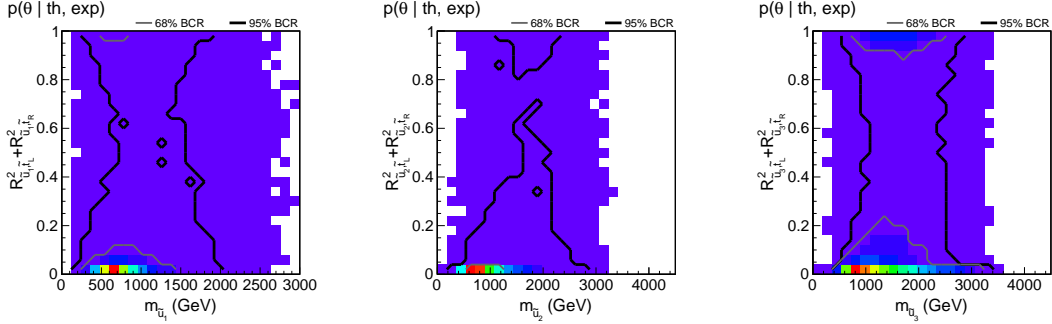


Figure 9. Resulting correlations between the stop flavour content and the masses of the three lightest up-type squarks after imposing all experimental constraints mentioned in Table 3. Red colour indicates the highest and dark purple the lowest likelihood.

lightest states are still found to be up-like or charm-like.

Similar conclusions hold for the sector of the down-type squarks. We show their masses in Figure 10 and selected flavour decompositions in Figure 11. The three lighter states exhibit comparable distributions, peaking as for the up-type squarks at about 800–1000 GeV. The mass distributions of the \tilde{d}_4 and \tilde{d}_5 states feature distributions with a larger spread, and the one of heaviest \tilde{d}_6 squark is peaking at about 3 TeV, although masses of about 1 TeV are predicted for a small subset of scenarios. Flavour mixing in the down-type squark sector is generally less pronounced than for the up-type squarks, as illustrated on Figure 11

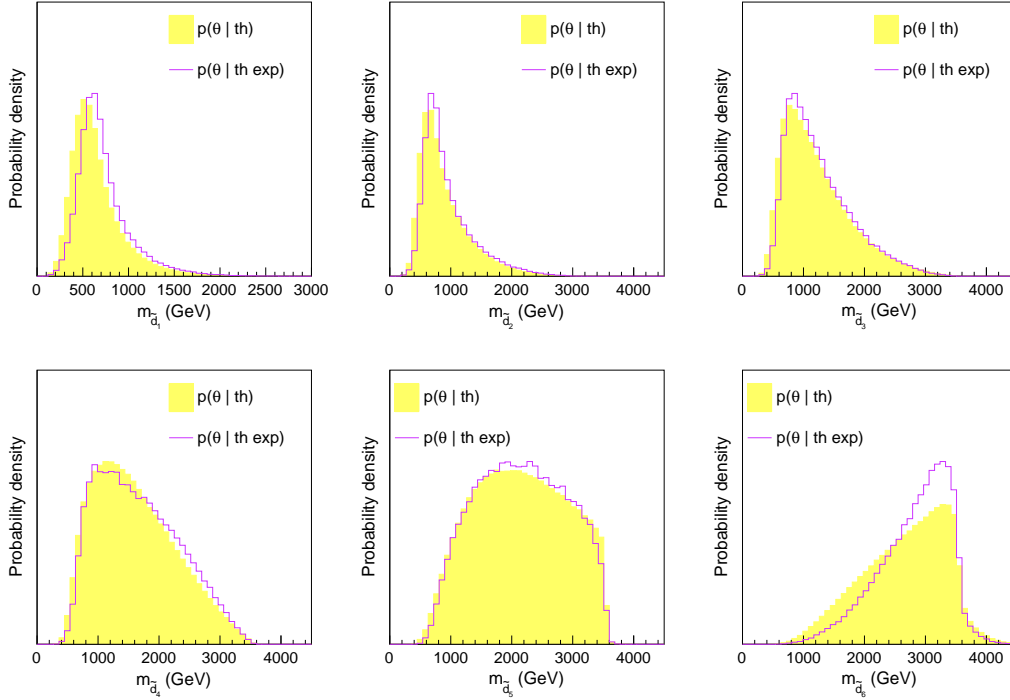


Figure 10. Same as Figure 8 for the down-type squark sector.

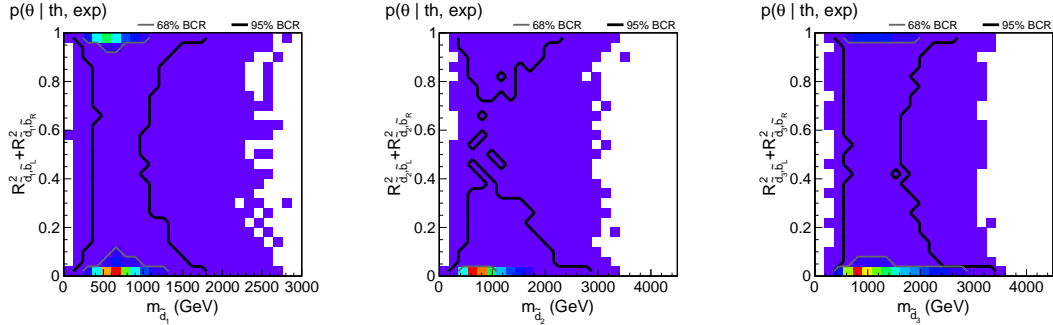


Figure 11. Resulting correlations between the sbottom flavour content and the masses of the three lightest down-type squarks after imposing all experimental constraints mentioned in Table 3. Red colour indicates the highest and dark purple the lowest likelihood.

where we depict the correlations between the sbottom content and the masses of the lighter down-type squarks. A majority of scenarios include light down-like and strange-like squark states and there is only a small number of parameter points where \tilde{d}_1 and \tilde{d}_2 contain a sizeable sbottom content.

In Figure 12, we show the correlations between the masses of the lightest squark states and the one of the lightest neutralino. For most ($\sim 95\%$) viable points, the mass difference is well above 50 GeV, which is a favorable condition for collider searches as the spectrum is not compressed. A considerable number ($\sim 40\%$) of parameter points features \tilde{u}_1 masses of about 500 – 1000 GeV together with neutralino masses of the order of 150 – 400 GeV.

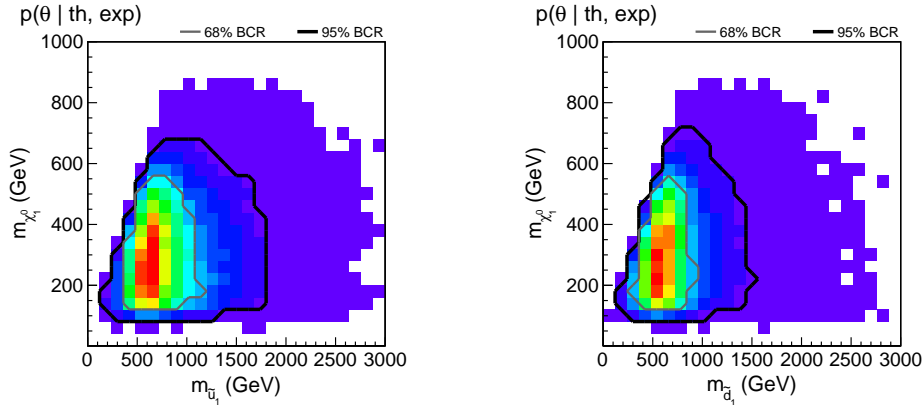


Figure 12. Correlations between the lightest neutralino mass and the lightest up- and down-type squark masses. Red colour indicates the highest likelihood.

Such mass configurations are likely to be ruled out by Run I LHC data. This is accounted for in the next section, where we include collider constraints on the NMFV MSSM setup and define benchmark scenarios suitable for searches at the LHC Run II.

5 Benchmark scenarios

In this section, we identify an ensemble of benchmark scenarios capturing typical features of the parameter space regions favoured by the constraints previously investigated. We have ordered all acceptable parameter setups according to their likelihood and selected four scenarios among the best ones. Our selection is aimed to cover different phenomenological properties of the NMFV MSSM and to be relevant for future LHC searches. The input parameters corresponding to the benchmark scenarios of our choice are indicated in Table 5. In Figure 13, we present the mass spectra of the four selected scenarios and depict the flavour content of the different squark eigenstates. We finally show in Table 6 the branching ratios related to the dominant decay modes of the squarks lighter than about 1 TeV. Additionally, we have verified that the electroweak vacuum is stable for all selected points by using the programme `Vevacious` [77]. We now briefly outline the main characteristics of the four proposed benchmark scenarios².

Scenario I This benchmark point presents one up-type and two down-type squarks with masses below 1 TeV. The lightest up-type squark is mostly stop-like, although it contains a small scharm component, and has a mass of 831 GeV which implies a sizeable production cross section at the LHC. In the sector of the down-type squarks, the two lightest states are almost purely sbottom-like with masses of 763 GeV and 854 GeV respectively. Since only the heaviest neutralino and chargino states are heavier than the three lightest squark states, various decay channels are open so that the real challenge for future LHC analyses would be to become sensitive to flavour-violating branching ratios of a few percents. In

²The benchmark scenarios can be provided, under the form of Supersymmetry Les Houches Accord compliant files [78], by the authors upon request.

Parameter	I	II	III	IV
$\alpha_s(m_Z)$	$1.187 \cdot 10^{-1}$	$1.194 \cdot 10^{-1}$	$1.176 \cdot 10^{-1}$	$1.176 \cdot 10^{-1}$
m_t^{pole}	176.00 GeV	175.53 GeV	173.53 GeV	174.02 GeV
$m_b(m_b)$	4.10 GeV	4.24 GeV	4.28 GeV	4.10 GeV
$M_{\tilde{Q}_{1,2}}$	1192.7 GeV	2288.2 GeV	637.7 GeV	753.2 GeV
$M_{\tilde{Q}_3}$	883.7 GeV	425.3 GeV	3483.0 GeV	2662.7 GeV
$M_{\tilde{U}_{1,2}}$	2412.6 GeV	1757.7 GeV	934.0 GeV	984.7 GeV
$M_{\tilde{U}_3}$	2344.3 GeV	2753.8 GeV	2862.2 GeV	2010.6 GeV
$M_{\tilde{D}_{1,2}}$	2295.1 GeV	551.6 GeV	1331.1 GeV	882.7 GeV
$M_{\tilde{D}_3}$	843.8 GeV	713.5 GeV	901.8 GeV	670.5 GeV
A_f	-2424.1 GeV	1807.3 GeV	1586.3 GeV	-2833.4 GeV
$\tan \beta$	17.4	21.1	29.2	34.0
μ	615.7 GeV	772.8 GeV	508.1 GeV	442.7 GeV
m_A	1334.5 GeV	1300.3 GeV	1294.8 GeV	1431.0 GeV
M_1	474.5 GeV	315.3 GeV	525.2 GeV	390.0 GeV
$M_{\tilde{\ell}}$	2466.5 GeV	1552.5 GeV	3396.7 GeV	2813.4 GeV
δ_{LL}	$1.4 \cdot 10^{-1}$	$-4.6 \cdot 10^{-2}$	$3.7 \cdot 10^{-1}$	$5.9 \cdot 10^{-1}$
δ_{RR}^u	$1.7 \cdot 10^{-1}$	$2.2 \cdot 10^{-1}$	$7.3 \cdot 10^{-1}$	$6.0 \cdot 10^{-1}$
δ_{RR}^d	$1.4 \cdot 10^{-1}$	$-1.4 \cdot 10^{-1}$	$-2.9 \cdot 10^{-1}$	$-7.5 \cdot 10^{-1}$
δ_{LR}^u	$9.2 \cdot 10^{-2}$	$3.5 \cdot 10^{-2}$	$1.7 \cdot 10^{-1}$	$1.0 \cdot 10^{-1}$
δ_{LR}^d	$-3.9 \cdot 10^{-2}$	$-3.6 \cdot 10^{-3}$	$-6.1 \cdot 10^{-3}$	$4.6 \cdot 10^{-3}$
δ_{RL}^u	$-9.7 \cdot 10^{-2}$	$1.4 \cdot 10^{-2}$	$-9.9 \cdot 10^{-2}$	$-7.2 \cdot 10^{-2}$
δ_{RL}^d	$-7.6 \cdot 10^{-4}$	$-1.4 \cdot 10^{-2}$	$-1.2 \cdot 10^{-3}$	$1.6 \cdot 10^{-3}$

Table 5. Definition of four benchmark points suitable for phenomenological studies of the NMFV MSSM.

this scenario, the electroweak vacuum is long-lived and has a lifetime larger than the age of the Universe.

Scenario II In this scenario, only the lightest of the up-type squarks is expected to lie within the reach of LHC, with a mass of 526 GeV. It is almost a pure stop state with a small charm component. Since the only lighter superpartner is the lightest neutralino, it will preferably decay into a $\tilde{\chi}_1^0 t$ system. There are four down-type squarks lying below 1 TeV, their masses being 519 GeV, 555 GeV, 566 GeV and 747 GeV. These four states are admixtures of all three flavours and their dominant decay modes include in particular final states containing the next-to-lightest neutralino or the lightest chargino. Contrary

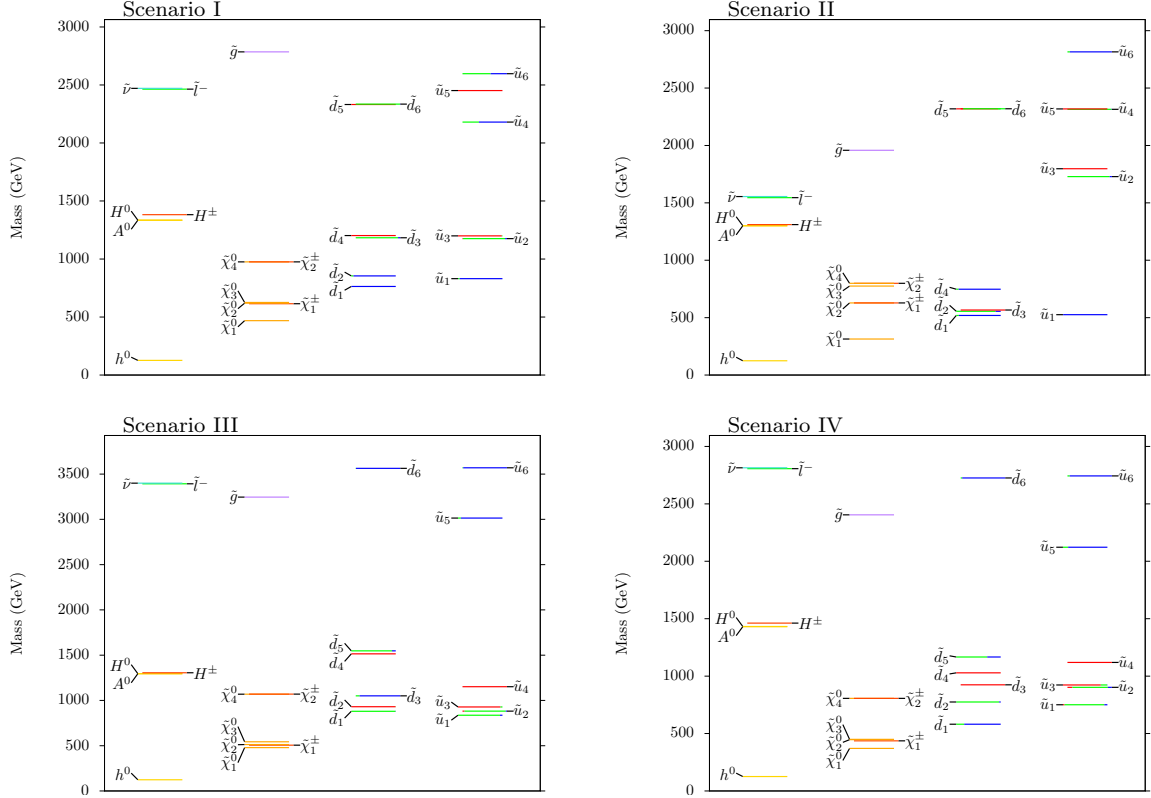


Figure 13. Mass spectra of the benchmark scenarios defined in Table 5. The colour code that has been employed for depicting the squark eigenstates indicates their flavour content: the {red, green, blue} colour corresponds to the {first, second, third} generation flavours.

to the scenario I, the branching ratios related to flavour-violating decays can reach up to 16 percents, which make them possibly testable at the LHC. Moreover, the fourth down-type squark has sizeable branching ratios for decays into the lightest up-type squark and a W -boson as well as into the lightest down-type squark and either a Z -boson or a Higgs boson. Although many squarks are very light, this scenario evades all LHC Run I constraints thanks to a heavy lightest neutralino of 315 GeV. Moreover, the vacuum has been found to be stable.

Scenario III This benchmark point features numerous squark mass eigenstates in the reach of the LHC. It indeed exhibits three up-type squarks with masses of 836 GeV, 882 GeV and 928 GeV, and three down-type squarks with masses of 880 GeV, 931 GeV and 1050 GeV. The stop-like states are here the heaviest ones, and the up-type squark states reachable at LHC only contain up and charm flavours. Similarly, the heavier \tilde{d}_3 and \tilde{d}_6 down-type squarks are the only ones containing a sbottom component. This feature is the direct consequence of the lower values that are favoured for the $M_{\tilde{Q}_{1,2}}$, $M_{\tilde{U}_{1,2}}$ and $M_{\tilde{D}_{1,2}}$ parameters, when compared to the values that are favoured by the third-generation soft parameters $M_{\tilde{Q}_3}$, $M_{\tilde{U}_3}$ and $M_{\tilde{D}_3}$. Equivalently, this can be seen as an implication of allowing for flavour-violating entries in the squark mass matrices (see Section 4.1). In

Decay	I	II	III	IV	Decay	I	II	III	IV
$\tilde{u}_1 \rightarrow t\tilde{\chi}_1^0$	0.14	0.99	0.06	0.09	$\tilde{d}_1 \rightarrow b\tilde{\chi}_1^0$	0.73	0.84		0.35
$\tilde{u}_1 \rightarrow c\tilde{\chi}_1^0$		0.01	0.24	0.07	$\tilde{d}_1 \rightarrow s\tilde{\chi}_1^0$		0.16	0.40	0.09
$\tilde{u}_1 \rightarrow t\tilde{\chi}_2^0$	0.24		0.11		$\tilde{d}_1 \rightarrow b\tilde{\chi}_2^0$	0.15		0.01	0.30
$\tilde{u}_1 \rightarrow t\tilde{\chi}_3^0$	0.43		0.06	0.26	$\tilde{d}_1 \rightarrow s\tilde{\chi}_2^0$			0.02	
$\tilde{u}_1 \rightarrow t\tilde{\chi}_3^0$				0.07	$\tilde{d}_1 \rightarrow b\tilde{\chi}_3^0$	0.12			0.25
$\tilde{u}_1 \rightarrow c\tilde{\chi}_3^0$			0.27	0.10	$\tilde{d}_1 \rightarrow s\tilde{\chi}_3^0$			0.05	
$\tilde{u}_1 \rightarrow b\tilde{\chi}_1^+$	0.19		0.24	0.22	$\tilde{d}_1 \rightarrow t\tilde{\chi}_1^-$			0.42	
$\tilde{u}_1 \rightarrow s\tilde{\chi}_1^+$			0.02	0.17	$\tilde{d}_1 \rightarrow c\tilde{\chi}_1^-$			0.09	
$\tilde{u}_1 \rightarrow W^+ \tilde{d}_1$				0.02	$\tilde{d}_2 \rightarrow b\tilde{\chi}_1^0$	0.04	0.05		0.02
$\tilde{u}_2 \rightarrow t\tilde{\chi}_1^0$			0.07	0.04	$\tilde{d}_2 \rightarrow s\tilde{\chi}_1^0$				0.24
$\tilde{u}_2 \rightarrow c\tilde{\chi}_1^0$			0.22	0.32	$\tilde{d}_2 \rightarrow d\tilde{\chi}_1^0$			0.70	
$\tilde{u}_2 \rightarrow t\tilde{\chi}_2^0$			0.08	0.09	$\tilde{d}_2 \rightarrow b\tilde{\chi}_2^0$				0.04
$\tilde{u}_2 \rightarrow t\tilde{\chi}_3^0$			0.09	0.11	$\tilde{d}_2 \rightarrow s\tilde{\chi}_2^0$	0.04	0.95		
$\tilde{u}_2 \rightarrow c\tilde{\chi}_3^0$			0.35	0.06	$\tilde{d}_2 \rightarrow d\tilde{\chi}_2^0$			0.03	
$\tilde{u}_2 \rightarrow b\tilde{\chi}_1^+$			0.11	0.21	$\tilde{d}_2 \rightarrow d\tilde{\chi}_2^0$			0.08	
$\tilde{u}_2 \rightarrow s\tilde{\chi}_1^+$			0.09		$\tilde{d}_2 \rightarrow b\tilde{\chi}_3^0$				0.04
$\tilde{u}_2 \rightarrow W^+ \tilde{d}_2$				0.06	$\tilde{d}_2 \rightarrow s\tilde{\chi}_3^0$	0.04			0.02
$\tilde{u}_2 \rightarrow Z^0 \tilde{u}_1$				0.05	$\tilde{d}_2 \rightarrow t\tilde{\chi}_1^-$	0.87			0.51
$\tilde{u}_2 \rightarrow h^0 \tilde{u}_1$				0.02	$\tilde{d}_2 \rightarrow c\tilde{\chi}_1^-$				0.09
$\tilde{u}_3 \rightarrow c\tilde{\chi}_1^0$			0.03	0.09	$\tilde{d}_2 \rightarrow u\tilde{\chi}_1^-$			0.15	
$\tilde{u}_3 \rightarrow u\tilde{\chi}_1^0$			0.03	0.03	$\tilde{d}_2 \rightarrow W^- \tilde{u}_1$			0.03	
$\tilde{u}_3 \rightarrow t\tilde{\chi}_2^0$				0.02	$\tilde{d}_2 \rightarrow Z^0 \tilde{d}_1$				0.02
$\tilde{u}_3 \rightarrow t\tilde{\chi}_3^0$				0.02	$\tilde{d}_2 \rightarrow h^0 \tilde{d}_1$				0.02
$\tilde{u}_3 \rightarrow c\tilde{\chi}_3^0$			0.05	0.02	$\tilde{d}_3 \rightarrow d\tilde{\chi}_1^0$		1.00		0.16
$\tilde{u}_3 \rightarrow u\tilde{\chi}_3^0$			0.45	0.09	$\tilde{d}_3 \rightarrow d\tilde{\chi}_3^0$				0.01
$\tilde{u}_3 \rightarrow c\tilde{\chi}_4^0$				0.01	$\tilde{d}_3 \rightarrow d\tilde{\chi}_4^0$				0.25
$\tilde{u}_3 \rightarrow u\tilde{\chi}_4^0$				0.15	$\tilde{d}_3 \rightarrow u\tilde{\chi}_1^-$				0.07
$\tilde{u}_3 \rightarrow b\tilde{\chi}_1^+$			0.01	0.05	$\tilde{d}_3 \rightarrow c\tilde{\chi}_2^-$				0.02
$\tilde{u}_3 \rightarrow d\tilde{\chi}_1^+$			0.41	0.01	$\tilde{d}_3 \rightarrow u\tilde{\chi}_2^-$				0.48
$\tilde{u}_3 \rightarrow d\tilde{\chi}_2^+$				0.33	$\tilde{d}_4 \rightarrow b\tilde{\chi}_1^0$		0.42		
$\tilde{u}_3 \rightarrow W^+ \tilde{d}_2$				0.01	$\tilde{d}_4 \rightarrow s\tilde{\chi}_1^0$		0.03		
$\tilde{u}_3 \rightarrow Z^0 \tilde{u}_1$				0.02	$\tilde{d}_4 \rightarrow d\tilde{\chi}_1^0$				0.83
					$\tilde{d}_4 \rightarrow d\tilde{\chi}_3^0$				0.17
					$\tilde{d}_4 \rightarrow W^- \tilde{u}_1$		0.27		
					$\tilde{d}_4 \rightarrow Z^0 \tilde{d}_1$		0.13		
					$\tilde{d}_4 \rightarrow h^0 \tilde{d}_1$		0.13		
					$\tilde{d}_4 \rightarrow h^0 \tilde{d}_2$		0.01		

Table 6. Branching ratios associated with the dominant decay modes of the up-type (left) and down-type (right) squarks lighter than about 1 TeV for the benchmark points defined in Table 5. Branching ratios below 1% are not indicated.

addition, all gauginos except the heaviest neutralino and chargino feature lower masses, so that a variety of decay channels are open. Finally, we found a direction in which, for extremely large field excitations, the electroweak vacuum is unbounded from below. This situation is similar to the case of the Standard Model [79, 80], and higher order corrections to the scalar potential would be needed to make a conclusive statement.

Scenario IV Our last scenario features numerous squark states as well as a complete electroweakino spectrum below 1 TeV. More precisely, the lighter up-type squarks have masses of 751 GeV, 902 GeV and 923 GeV, while the lighter down-type squark masses are of 582 GeV, 775 GeV and 924 GeV. In addition, three other states are not too far above 1 TeV with masses of 1119 GeV (\tilde{u}_4), 1029 GeV (\tilde{d}_4) and 1167 GeV (\tilde{d}_5). The two lightest up-type squarks consist in this case of a mixture of all three flavours (with a dominant charm content), which leads to interesting decay patterns, as shown in Table 6. Similarly to scenario I, this scenario exhibits a long-lived electroweak vacuum with a lifetime larger than the age of the Universe.

6 Conclusion

We have studied non-minimal flavour-violation in the MSSM by allowing for flavour mixing between the second and third generation squarks. We have used a Markov Chain Monte Carlo scanning technique to explore the underlying parameter space and imposed a set of experimental constraints arising from B -meson and kaon physics. We have additionally enforced the model to accommodate a light Higgs boson with a mass of 125 GeV.

First and second generation soft squark masses are theoretically restricted to low values in order to avoid tachyons in the Higgs sector. As a consequence, the lighter squarks are often not the stop and sbottom ones, which contrasts with scenarios of the usual minimally flavour-violating MSSM. Requiring a theoretically consistent Higgs sector and a light Higgs boson of about 125 GeV similarly restrict the left-right and right-left flavour-violating squark mixing parameters $\delta_{LR/RL}^{u,d}$ to be small. In contrast, the δ_{LL} and δ_{RR}^d NMFV parameters are mainly constrained by neutral B -meson oscillations, and the rare $B_s \rightarrow \mu\mu$ decay mainly influences δ_{RL}^u . All other NMFV parameters are left unconstrained by the considered experimental observations.

In view of the recently started second LHC run, we have used our MCMC scan results to propose four benchmark scenarios allowed by current data that exhibit distinct features and that are suitable for future analyses of NMFV effects in the MSSM. In most proposed scenarios, several squarks have masses close to 1 TeV so that they should be reachable within the next few years.

Acknowledgments

The authors would like to thank the organisers of the ‘PhysTeV Les Houches’ workshop, where this work has been initiated, for the welcoming and inspiring atmosphere. We are also grateful to the IIHE IT team for allowing us to use the IIHE cluster. KDC and NS are supported in part by ‘FWO-Vlaanderen’ aspirant fellowships, and KDC also thanks the

Strategic Research Program ‘High Energy Physics’ of the Vrije Universiteit Brussel. BF and FM acknowledge partial support from the Theory-LHC France initiative of the CNRS (IN2P3/INP) and WP has been supported by the BMBF, project nr. 05H12WWE.

References

- [1] H. P. Nilles, *Supersymmetry, Supergravity and Particle Physics*, *Phys.Rept.* **110** (1984) 1–162.
- [2] H. E. Haber and G. L. Kane, *The Search for Supersymmetry: Probing Physics Beyond the Standard Model*, *Phys.Rept.* **117** (1985) 75–263.
- [3] <http://twiki.cern.ch/twiki/AtlasPublic/SupersymmetryPublicResults>.
- [4] <http://twiki.cern.ch/twiki/CMSPublic/PhysicsResultsSUS>.
- [5] L. J. Hall, V. A. Kostelecky, and S. Raby, *New Flavor Violations in Supergravity Models*, *Nucl.Phys.* **B267** (1986) 415.
- [6] G. D’Ambrosio, G. Giudice, G. Isidori, and A. Strumia, *Minimal flavor violation: An Effective field theory approach*, *Nucl.Phys.* **B645** (2002) 155–187, [[hep-ph/0207036](#)].
- [7] V. Cirigliano, B. Grinstein, G. Isidori, and M. B. Wise, *Minimal flavor violation in the lepton sector*, *Nucl.Phys.* **B728** (2005) 121–134, [[hep-ph/0507001](#)].
- [8] F. Gabbiani and A. Masiero, *FCNC in Generalized Supersymmetric Theories*, *Nucl.Phys.* **B322** (1989) 235.
- [9] M. Artuso, D. Asner, P. Ball, E. Baracchini, G. Bell, et al., *B, D and K decays*, *Eur.Phys.J.* **C57** (2008) 309–492, [[arXiv:0801.1833](#)].
- [10] S. Heinemeyer, W. Hollik, F. Merz, and S. Penaranda, *Electroweak precision observables in the MSSM with nonminimal flavor violation*, *Eur.Phys.J.* **C37** (2004) 481–493, [[hep-ph/0403228](#)].
- [11] G. Bozzi, B. Fuks, B. Herrmann, and M. Klasen, *Squark and gaugino hadroproduction and decays in non-minimal flavour violating supersymmetry*, *Nucl.Phys.* **B787** (2007) 1–54, [[arXiv:0704.1826](#)].
- [12] S. Dittmaier, G. Hiller, T. Plehn, and M. Spannowsky, *Charged-Higgs Collider Signals with or without Flavor*, *Phys. Rev.* **D77** (2008) 115001, [[arXiv:0708.0940](#)].
- [13] B. Fuks, B. Herrmann, and M. Klasen, *Flavour Violation in Gauge-Mediated Supersymmetry Breaking Models: Experimental Constraints and Phenomenology at the LHC*, *Nucl.Phys.* **B810** (2009) 266–299, [[arXiv:0808.1104](#)].
- [14] T. Hurth and W. Porod, *Flavour violating squark and gluino decays*, *JHEP* **0908** (2009) 087, [[arXiv:0904.4574](#)].
- [15] A. Bartl et al., *Impact of squark generation mixing on the search for gluinos at LHC*, *Phys.Lett.* **B679** (2009) 260–266, [[arXiv:0905.0132](#)].
- [16] T. Plehn, M. Rauch, and M. Spannowsky, *Understanding Single Tops using Jets*, *Phys. Rev.* **D80** (2009) 114027, [[arXiv:0906.1803](#)].
- [17] A. Bartl et al., *Impact of squark generation mixing on the search for squarks decaying into fermions at LHC*, *Phys.Lett.* **B698** (2011) 380–388, [[arXiv:1007.5483](#)].
- [18] M. Bruhnke, B. Herrmann, and W. Porod, *Signatures of bosonic squark decays in non-minimally flavour-violating supersymmetry*, *JHEP* **1009** (2010) 006, [[arXiv:1007.2100](#)].
- [19] A. Bartl et al., *Flavour violating gluino three-body decays at LHC*, *Phys.Rev.* **D84** (2011) 115026, [[arXiv:1107.2775](#)].

- [20] B. Fuks, B. Herrmann, and M. Klasen, *Phenomenology of anomaly-mediated supersymmetry breaking scenarios with non-minimal flavour violation*, *Phys.Rev.* **D86** (2012) 015002, [[arXiv:1112.4838](#)].
- [21] A. Bartl, H. Eberl, E. Ginina, B. Herrmann, K. Hidaka, et al., *Flavor violating bosonic squark decays at LHC*, *Int.J.Mod.Phys.* **A29** (2014) 1450035, [[arXiv:1212.4688](#)].
- [22] M. Blanke, G. F. Giudice, P. Paradisi, G. Perez, and J. Zupan, *Flavoured Naturalness*, *JHEP* **1306** (2013) 022, [[arXiv:1302.7232](#)].
- [23] J. Aebischer, A. Crivellin, and C. Greub, *One-loop SQCD corrections to the decay of top squarks to charm and neutralino in the generic MSSM*, *Phys. Rev.* **D91** (2015), no. 3 035010, [[arXiv:1410.8459](#)].
- [24] M. Backovi, A. Mariotti, and M. Spannowsky, *Signs of Tops from Highly Mixed Stops*, *JHEP* **06** (2015) 122, [[arXiv:1504.0092](#)].
- [25] M. Arana-Catania, S. Heinemeyer, and M. Herrero, *Updated Constraints on General Squark Flavor Mixing*, *Phys.Rev.* **D90** (2014), no. 7 075003, [[arXiv:1405.6960](#)].
- [26] K. Kowalska, *Phenomenology of SUSY with General Flavour Violation*, *JHEP* **1409** (2014) 139, [[arXiv:1406.0710](#)].
- [27] M. Ciuchini, A. Masiero, P. Paradisi, L. Silvestrini, S. Vempati, et al., *Soft SUSY breaking grand unification: Leptons versus quarks on the flavor playground*, *Nucl.Phys.* **B783** (2007) 112–142, [[hep-ph/0702144](#)].
- [28] F. Gabbiani, E. Gabrielli, A. Masiero, and L. Silvestrini, *A Complete analysis of FCNC and CP constraints in general SUSY extensions of the standard model*, *Nucl.Phys.* **B477** (1996) 321–352, [[hep-ph/9604387](#)].
- [29] **Particle Data Group** Collaboration, J. Beringer et al., *Review of Particle Physics (RPP)*, *Phys.Rev.* **D86** (2012) 010001.
- [30] W. Porod, *SPheno, a program for calculating supersymmetric spectra, SUSY particle decays and SUSY particle production at e^+e^- colliders*, *Comput.Phys.Commun.* **153** (2003) 275–315, [[hep-ph/0301101](#)].
- [31] W. Porod and F. Staub, *SPheno 3.1: Extensions including flavour, CP-phases and models beyond the MSSM*, *Comput.Phys.Commun.* **183** (2012) 2458–2469, [[arXiv:1104.1573](#)].
- [32] A. A. Markov, *Extension of the limit theorems of probability theory to a sum of variables connected in a chain*. reprinted in Appendix B of: R. Howard, *Dynamic Probabilistic Systems, volume 1: Markov Chains*, John Wiley and Sons, 1971.
- [33] N. Metropolis, A. W. Rosenbluth, M. N. Rosenbluth, A. H. Teller, and E. Teller, *Equation of state calculations by fast computing machines*, *J. Chem. Phys.* **21** (1953) 1087–1092.
- [34] W. K. Hastings, *Monte Carlo Sampling Methods Using Markov Chains and Their Applications*, *Biometrika* **57** (1970) 97–109.
- [35] **Heavy Flavor Averaging Group (HFAG)** Collaboration, Y. Amhis et al., *Averages of b -hadron, c -hadron, and τ -lepton properties as of summer 2014*, [[arXiv:1412.7515](#)].
- [36] **LHCb, CMS** Collaboration, V. Khachatryan et al., *Observation of the rare $B^0_{-s} \rightarrow \mu^+ \mu^-$ decay from the combined analysis of CMS and LHCb data*, *Nature* **522** (2015) 68–72, [[arXiv:1411.4413](#)].

- [37] **LHCb** Collaboration, R. Aaij et al., *Differential branching fraction and angular analysis of the decay $B^0 \rightarrow K^{*0} \mu^+ \mu^-$* , *JHEP* **1308** (2013) 131, [[arXiv:1304.6325](#)].
- [38] **LHCb** Collaboration, *Angular analysis of the $B^0 \rightarrow K^{*0} \mu^+ \mu^-$ decay*, LHCb-CONF-2015-002, CERN-LHCb-CONF-2015-002.
- [39] **BaBar** Collaboration, J. Lees et al., *Measurement of the $B \rightarrow X_s \ell^+ \ell^-$ branching fraction and search for direct CP violation from a sum of exclusive final states*, *Phys.Rev.Lett.* **112** (2014) 211802, [[arXiv:1312.5364](#)].
- [40] **ATLAS** Collaboration, G. Aad et al., *Observation of a new particle in the search for the Standard Model Higgs boson with the ATLAS detector at the LHC*, *Phys.Lett.* **B716** (2012) 1–29, [[arXiv:1207.7214](#)].
- [41] **CMS** Collaboration, S. Chatrchyan et al., *Observation of a new boson at a mass of 125 GeV with the CMS experiment at the LHC*, *Phys.Lett.* **B716** (2012) 30–61, [[arXiv:1207.7235](#)].
- [42] F. Mahmoudi, *SuperIso: A Program for calculating the isospin asymmetry of $B \rightarrow K^* \gamma$ in the MSSM*, *Comput.Phys.Commun.* **178** (2008) 745–754, [[arXiv:0710.2067](#)].
- [43] F. Mahmoudi, *SuperIso v2.3: A Program for calculating flavor physics observables in Supersymmetry*, *Comput.Phys.Commun.* **180** (2009) 1579–1613, [[arXiv:0808.3144](#)].
- [44] F. Mahmoudi, S. Heinemeyer, A. Arbey, A. Bharucha, T. Goto, et al., *Flavour Les Houches Accord: Interfacing Flavour related Codes*, *Comput.Phys.Commun.* **183** (2012) 285–298, [[arXiv:1008.0762](#)].
- [45] M. Misiak, H. Asatrian, K. Bieri, M. Czakon, A. Czarnecki, et al., *Estimate of $B(\bar{B} \rightarrow X(s)\gamma)$ at $O(\alpha(s)^2)$* , *Phys.Rev.Lett.* **98** (2007) 022002, [[hep-ph/0609232](#)].
- [46] M. Misiak and M. Steinhauser, *NNLO QCD corrections to the $\bar{B} \rightarrow X_s \gamma$ matrix elements using interpolation in $m(c)$* , *Nucl.Phys.* **B764** (2007) 62–82, [[hep-ph/0609241](#)].
- [47] M. Misiak and M. Poradzinski, *Completing the Calculation of BLM corrections to $\bar{B} \rightarrow X_s \gamma$* , *Phys.Rev.* **D83** (2011) 014024, [[arXiv:1009.5685](#)].
- [48] Y.-B. Dai, C.-S. Huang, and H.-W. Huang, *$B \rightarrow X_s \tau^+ \tau^-$ in a two Higgs doublet model*, *Phys.Lett.* **B390** (1997) 257–262, [[hep-ph/9607389](#)].
- [49] A. Ghinculov, T. Hurth, G. Isidori, and Y. Yao, *The Rare decay $B \rightarrow X_s l^+ l^-$ to NNLL precision for arbitrary dilepton invariant mass*, *Nucl.Phys.* **B685** (2004) 351–392, [[hep-ph/0312128](#)].
- [50] T. Huber, E. Lunghi, M. Misiak, and D. Wyler, *Electromagnetic logarithms in $\bar{B} \rightarrow X_s l^+ l^-$* , *Nucl.Phys.* **B740** (2006) 105–137, [[hep-ph/0512066](#)].
- [51] T. Huber, T. Hurth, and E. Lunghi, *Logarithmically Enhanced Corrections to the Decay Rate and Forward Backward Asymmetry in $\bar{B} \rightarrow X_s \ell^+ \ell^-$* , *Nucl.Phys.* **B802** (2008) 40–62, [[arXiv:0712.3009](#)].
- [52] M. Beneke, T. Feldmann, and D. Seidel, *Systematic approach to exclusive $B \rightarrow V l^+ l^-$, $V \gamma$ decays*, *Nucl.Phys.* **B612** (2001) 25–58, [[hep-ph/0106067](#)].
- [53] M. Beneke, T. Feldmann, and D. Seidel, *Exclusive radiative and electroweak $b \rightarrow d$ and $b \rightarrow s$ penguin decays at NLO*, *Eur.Phys.J.* **C41** (2005) 173–188, [[hep-ph/0412400](#)].
- [54] F. Kruger and J. Matias, *Probing new physics via the transverse amplitudes of $B^0 \rightarrow K^{*0}(\rightarrow K^- \pi^+) l^+ l^-$ at large recoil*, *Phys.Rev.* **D71** (2005) 094009, [[hep-ph/0502060](#)].

- [55] U. Egede, T. Hurth, J. Matias, M. Ramon, and W. Reece, *New observables in the decay mode $\bar{B}_d \rightarrow \bar{K}^{*0} \ell^+ \ell^-$* , *JHEP* **0811** (2008) 032, [[arXiv:0807.2589](#)].
- [56] U. Egede, T. Hurth, J. Matias, M. Ramon, and W. Reece, *New physics reach of the decay mode $\bar{B} \rightarrow \bar{K}^{*0} \ell^+ \ell^-$* , *JHEP* **1010** (2010) 056, [[arXiv:1005.0571](#)].
- [57] A. Khodjamirian, T. Mannel, A. Pivovarov, and Y.-M. Wang, *Charm-loop effect in $B \rightarrow K^{(*)} \ell^+ \ell^-$ and $B \rightarrow K^* \gamma$* , *JHEP* **1009** (2010) 089, [[arXiv:1006.4945](#)].
- [58] H. Dreiner, K. Nickel, W. Porod, and F. Staub, *Full 1-loop calculation of $BR(B_{s,d}^0 \rightarrow \ell \bar{\ell})$ in models beyond the MSSM with SARAH and SPheno*, *Comput.Phys.Commun.* **184** (2013) 2604–2617, [[arXiv:1212.5074](#)].
- [59] A. J. Buras, P. H. Chankowski, J. Rosiek, and L. Slawianowska, *$\Delta M_{d,s}, B^0 d, s \rightarrow \mu^+ \mu^-$ and $B \rightarrow X_s \gamma$ in supersymmetry at large $\tan \beta$* , *Nucl.Phys.* **B659** (2003) 3, [[hep-ph/0210145](#)].
- [60] G. Isidori and A. Retico, *$B_{s,d} \rightarrow \ell^+ \ell^-$ and $K_L \rightarrow \ell^+ \ell^-$ in SUSY models with nonminimal sources of flavor mixing*, *JHEP* **0209** (2002) 063, [[hep-ph/0208159](#)].
- [61] S. Baek, T. Goto, Y. Okada, and K.-i. Okumura, *Muon anomalous magnetic moment, lepton flavor violation, and flavor changing neutral current processes in SUSY GUT with right-handed neutrino*, *Phys.Rev.* **D64** (2001) 095001, [[hep-ph/0104146](#)].
- [62] A. J. Buras, S. Jager, and J. Urban, *Master formulae for Delta F=2 NLO QCD factors in the standard model and beyond*, *Nucl.Phys.* **B605** (2001) 600–624, [[hep-ph/0102316](#)].
- [63] S. Herrlich and U. Nierste, *The Complete $|\Delta S| = 2$ - Hamiltonian in the next-to-leading order*, *Nucl.Phys.* **B476** (1996) 27–88, [[hep-ph/9604330](#)].
- [64] A. J. Buras, T. Ewerth, S. Jager, and J. Rosiek, *$K^+ \rightarrow \pi^+ \nu \bar{\nu}$ and $K(L) \rightarrow \pi^0 \nu \bar{\nu}$ decays in the general MSSM*, *Nucl.Phys.* **B714** (2005) 103–136, [[hep-ph/0408142](#)].
- [65] G. Colangelo and G. Isidori, *Supersymmetric contributions to rare kaon decays: Beyond the single mass insertion approximation*, *JHEP* **9809** (1998) 009, [[hep-ph/9808487](#)].
- [66] A. Crivellin, L. Hofer, and J. Rosiek, *Complete resummation of chirally-enhanced loop-effects in the MSSM with non-minimal sources of flavor-violation*, *JHEP* **1107** (2011) 017, [[arXiv:1103.4272](#)].
- [67] T. Ibrahim and P. Nath, *CP violation and the muon anomaly in N=1 supergravity*, *Phys.Rev.* **D61** (2000) 095008, [[hep-ph/9907555](#)].
- [68] D. M. Pierce, J. A. Bagger, K. T. Matchev, and R.-j. Zhang, *Precision corrections in the minimal supersymmetric standard model*, *Nucl.Phys.* **B491** (1997) 3–67, [[hep-ph/9606211](#)].
- [69] G. Degrandi, P. Slavich, and F. Zwirner, *On the neutral Higgs boson masses in the MSSM for arbitrary stop mixing*, *Nucl.Phys.* **B611** (2001) 403–422, [[hep-ph/0105096](#)].
- [70] A. Brignole, G. Degrandi, P. Slavich, and F. Zwirner, *On the $O(\alpha(t)^2)$ two loop corrections to the neutral Higgs boson masses in the MSSM*, *Nucl.Phys.* **B631** (2002) 195–218, [[hep-ph/0112177](#)].
- [71] A. Brignole, G. Degrandi, P. Slavich, and F. Zwirner, *On the two loop sbottom corrections to the neutral Higgs boson masses in the MSSM*, *Nucl.Phys.* **B643** (2002) 79–92, [[hep-ph/0206101](#)].
- [72] A. Dedes, G. Degrandi, and P. Slavich, *On the two loop Yukawa corrections to the MSSM Higgs boson masses at large $\tan \beta$* , *Nucl.Phys.* **B672** (2003) 144–162, [[hep-ph/0305127](#)].

- [73] A. Dedes and P. Slavich, *Two loop corrections to radiative electroweak symmetry breaking in the MSSM*, *Nucl.Phys.* **B657** (2003) 333–354, [[hep-ph/0212132](#)].
- [74] B. Allanach, A. Djouadi, J. Kneur, W. Porod, and P. Slavich, *Precise determination of the neutral Higgs boson masses in the MSSM*, *JHEP* **0409** (2004) 044, [[hep-ph/0406166](#)].
- [75] M. Arana-Catania, S. Heinemeyer, M. Herrero, and S. Penaranda, *Higgs Boson masses and B-Physics Constraints in Non-Minimal Flavor Violating SUSY scenarios*, *JHEP* **1205** (2012) 015, [[arXiv:1109.6232](#)].
- [76] A. Gelman and D. B. Rubin, *Inference from iterative simulation using multiple sequences*, *Statist. Sci.* **7** (11, 1992) 457–472.
- [77] J. Camargo-Molina, B. O’Leary, W. Porod, and F. Staub, **Vevacious: A Tool For Finding The Global Minima Of One-Loop Effective Potentials With Many Scalars**, *Eur.Phys.J.* **C73** (2013) 2588, [[arXiv:1307.1477](#)].
- [78] B. C. Allanach et al., *SUSY Les Houches Accord 2*, *Comput. Phys. Commun.* **180** (2009) 8–25, [[arXiv:0801.0045](#)].
- [79] G. Degrandi, S. Di Vita, J. Elias-Miro, J. R. Espinosa, G. F. Giudice, et al., *Higgs mass and vacuum stability in the Standard Model at NNLO*, *JHEP* **1208** (2012) 098, [[arXiv:1205.6497](#)].
- [80] D. Buttazzo, G. Degrandi, P. P. Giardino, G. F. Giudice, F. Sala, et al., *Investigating the near-criticality of the Higgs boson*, *JHEP* **1312** (2013) 089, [[arXiv:1307.3536](#)].